The water vapour continuum in near-infrared windows – current understanding and prospects for its inclusion in spectroscopic databases

Journal of Molecular Spectroscopy 327 (2016) 193–208

Contents lists available at ScienceDirect

Journal of Molecular Spectroscopy

journal homepage: www.elsevier.com/locate/jms

The water vapour continuum in near-infrared windows – Current understanding and prospects for its inclusion in spectroscopic databases

Keith P. Shine [a,*], Alain Campargue [b,c], Didier Mondelain [b,c], Robert A. McPheat [d], Igor V. Ptashnik [e], Damien Weidmann [d]

[a] Department of Meteorology, University of Reading, Earley Gate, Reading RG6 6BB, UK
[b] Univ. Grenoble Alpes, LIPhy, F-38000 Grenoble, France
[c] CNRS, LIPhy, F-38000 Grenoble, France
[d] Space Science and Technology Department, Rutherford Appleton Laboratory, Chilton, Didcot, Oxon OX11 OQX, UK
[e] Spectroscopy Division, Zuev Institute of Atmospheric Optics SB RAS, 1 Akademichesky Av., Tomsk 634055, Russia

ARTICLE INFO

Article history:
Received 15 December 2015
In revised form 22 March 2016
Accepted 19 April 2016
Available online 20 April 2016

Keywords:
Water vapour
Absorption continuum
MT_CKD model
Water dimer

ABSTRACT

Spectroscopic catalogues, such as GEISA and HITRAN, do not yet include information on the water vapour continuum that pervades visible, infrared and microwave spectral regions. This is partly because, in some spectral regions, there are rather few laboratory measurements in conditions close to those in the Earth's atmosphere; hence understanding of the characteristics of the continuum absorption is still emerging. This is particularly so in the near-infrared and visible, where there has been renewed interest and activity in recent years. In this paper we present a critical review focusing on recent laboratory measurements in two near-infrared window regions (centred on 4700 and 6300 cm^{-1}) and include reference to the window centred on 2600 cm^{-1} where more measurements have been reported. The rather few available measurements, have used Fourier transform spectroscopy (FTS), cavity ring down spectroscopy, optical-feedback – cavity enhanced laser spectroscopy and, in very narrow regions, calorimetric interferometry. These systems have different advantages and disadvantages. Fourier Transform Spectroscopy can measure the continuum across both these and neighbouring windows; by contrast, the cavity laser techniques are limited to fewer wavenumbers, but have a much higher inherent sensitivity. The available results present a diverse view of the characteristics of continuum absorption, with differences in continuum strength exceeding a factor of 10 in the cores of these windows. In individual windows, the temperature dependence of the water vapour self-continuum differs significantly in the few sets of measurements that allow an analysis. The available data also indicate that the temperature dependence differs significantly between different near-infrared windows. These pioneering measurements provide an impetus for further measurements. Improvements and/or extensions in existing techniques would aid progress to a full characterisation of the continuum – as an example, we report pilot measurements of the water vapour self-continuum using a supercontinuum laser source coupled to an FTS. Such improvements, as well as additional measurements and analyses in other laboratories, would enable the inclusion of the water vapour continuum in future spectroscopic databases, and therefore allow for a more reliable forward modelling of the radiative properties of the atmosphere. It would also allow a more confident assessment of different theoretical descriptions of the underlying cause or causes of continuum absorption.

1. Introduction

Spectroscopic catalogues for atmospheric applications (notably GEISA [1] and HITRAN [2]) have reported the rotational and rotational–vibrational spectral line parameters across visible, infrared and microwave wavelength regions, as well as some cross-section data on broadband absorbers and collision-induced absorption [3]. However, they have not yet included information relevant to the water vapour continuum which pervades these same spectral regions. Instead, the default description of the water vapour continuum has generally been the semi-empirical Clough–Kneizys–Davies (CKD) continuum and its successor Mlawer–Tobin–CKD (MT_CKD) (see especially [4,5]). CKD and MT_CKD have

* Corresponding author.
E-mail address: k.p.shine@reading.ac.uk (K.P. Shine).

http://dx.doi.org/10.1016/j.jms.2016.04.011
0022-2852/

been widely used in atmospheric radiative transfer codes for applications including numerical weather prediction, climate modelling and remote sensing.

For understanding radiative fluxes in the Earth's atmosphere, it is the continuum in the windows between the dominant features in the water vapour spectrum (the pure rotational lines, at wavelengths less than 20 μm, and the many rotational–vibrational bands) that is of most significance. Within the main absorbing regions, continuum absorption is generally dominated by spectral-line absorption, with some exceptions. Although it may be of lesser importance in determining fluxes, the in-band continuum holds important clues as to the continuum's physical origin [6–8].

Historically, most attention has focused on the mid-infrared (800–1250 cm^{-1}, 8–12 μm) window (see [9] for references), which has a major influence on radiative fluxes (e.g. [10–12]), especially in atmospheres with high absolute humidity. To a lesser extent, the window centred on 2600 cm^{-1} (about 3.85 μm) has also been the subject of many studies (e.g. [13–16]). More recently, attention has begun to focus on several shorter wavelength near-infrared windows (which we define here to be 2500–14,300 cm^{-1} (0.7–4 μm)) where, prior to the year 2000, there were hardly any measurements. These windows are of atmospheric importance because they contain significant fluxes of solar radiation (e.g. [17]). They are also widely used for satellite-based sensing of gaseous abundances, notably carbon dioxide and methane (e.g. [18–20]), and cloud and surface properties (e.g. [21,22]).

In order to illustrate some of the issues that will have to be resolved before the water vapour continuum can be included in some form on spectroscopic databases, this paper particularly focuses on 2 of these windows, centred on about 6300 and 4700 cm^{-1} (1.6 and 2.1 μm). In these windows there have been a number of recent laboratory measurements which have highlighted important characteristics of the continuum absorption but also revealed significant and, as yet, unresolved disagreements. The nature of these disagreements, and prospects for future progress in resolving these, will be discussed with mention of the situation in other windows where appropriate.

2. Some characteristics of the water vapour continuum

2.1. Definitions

Since the work of Bignell [13] it has been clearly recognised that there are two distinct components to the water vapour continuum: (i) a self-continuum, which is interpreted as the interaction between water vapour molecules (such as collisions or the formation of some bound complex) and whose strength scales closely with the vapour pressure squared and (ii) a foreign-continuum, due to interaction of water vapour with other molecules, and most importantly molecular nitrogen and oxygen when considering the Earth's atmosphere. The foreign-continuum depends linearly on the water vapour pressure and on the foreign gas pressure.

As a result, the continuum absorption coefficient of water vapour in air, α_{WC}, is the sum of the self (WCS) and foreign (WCF) contributions so that

$$\alpha_{WC}(\nu,T) = \alpha_{WCS}(\nu,T) + \alpha_{WCF}(\nu,T) = \frac{1}{k_B T} C_S(\nu,T) P_{H_2O}^2 + \frac{1}{k_B T} C_F(\nu,T) P_{H_2O} P_F \quad (1)$$

where k_B is the Boltzmann constant, T is temperature, P_{H_2O} and P_F are the water vapour and foreign gas (here air) partial pressures, respectively, and C_S and C_F represent the self- and foreign-continuum cross-sections, respectively, at a given temperature T, following the definition in Burch and Alt [14]. In the standard units adopted in this field, C_S and C_F are reported in cm^2 $molec^{-1}$ atm^{-1}, α_{WC} is in cm^{-1}, P_{H_2O} and P_F are in atm, T is in K and $k_B = 1.36 \times 10^{-22}$ atm $molec^{-1}$ cm^3 K^{-1}. Note that for comparison, the MT_CKD values of C_S and C_F [5], which are normalised to the number density at 1 atm and 296 K, should be multiplied by the factor $296/T$ (e.g. [23]).

Most, but not all (see Sections 3.1 and 3.2), available measurements of the self-continuum cross-section show a strong negative temperature dependence. By contrast, within measurement and analysis uncertainties, the foreign continuum appears independent of temperature in the range from about 300 to 430 K (see Section 3.3).

There is no unambiguous way of defining the water vapour continuum, and separating it from smoothly varying line absorption. However, some operational definition is needed to enable comparison between observations and to allow implementation of the continuum in radiative transfer codes. The most widespread definition is that used by CKD and MT_CKD [4,5]. The line absorption is defined as the purely Lorentzian-broadened profile calculated above its value at 25 cm^{-1} from line centre. All line absorption further than 25 cm^{-1} from line centre, as well as the 25 cm^{-1} "pedestal" on which the line sits, is assumed to be part of the continuum (see Fig. 1 of [4]). At any wavenumber, the continuum is thus defined as the observed absorption that cannot be accounted for by line-by-line calculations using this assumed line profile for all lines within 25 cm^{-1} of that wavenumber. Using this definition, the derived continuum is not independent of the spectral line database used to derive it, and indeed should be updated as new information on water vapour lines (including all isotopologues) becomes available. However, in the near-infrared bands, the pedestal itself accounts for only 5–7% of the continuum, and it is much less important (around 1%) within the window regions (e.g. [24]) which are the focus here.

2.2. Theoretical overview

Since this paper focuses on the observational evidence for the characteristics of the water vapour continuum, we largely sidestep the issue of the underlying physical cause, or causes, of the water vapour continuum absorption, which remains a vigorously debated area; greater confidence, stemming from a larger set of independent, cross-validated, experimental data is essential to judge the success, or otherwise, of theoretical explanations, and to guide new developments. Nevertheless, a brief overview will help frame the discussion. Up to now, there have been broadly two main "competitor" explanations for the continuum, which should not be seen as mutually exclusive. Some history of the development of these ideas can be found in Ref. [9].

The first explanation is far-wing theory. The CKD and MT_CKD descriptions have been based on the semi-empirical adjustment to the Lorentz line shape of water vapour lines; the adjustment was derived so as to fit available observations of the continuum mostly at wavenumbers less than 2200 cm^{-1}. The resulting lineshape was then applied at all wavenumbers. In CKD, this adjustment led to both a super-Lorentzian component in the near-wing regions (10–100 cm^{-1} from line centre) with a sub-Lorentzian component beyond; the sub-Lorentzian component therefore dominates in the windows [4]. In MT_CKD, the super-Lorentzian component was replaced by a "weak interaction term" where the weak interaction is between a water vapour molecule with another molecule (which could itself be water vapour) [5]. A quite different approach to far-wing line theory has been presented by Ma et al. [25,26], which has a more *ab initio* basis,

but still ultimately requires empirical adjustment. A theoretical semi-classical approach has also been presented by Tvorogov and Rodimova [27] and developed in later work [28,29]. This approach is acquiring a more semi-empirical nature due to the need to specify, on the basis of available observations, a large number of *ad-hoc* fitting parameters.

The second interpretation is that water dimers are the cause of the continuum (see e.g. recent reviews by [6–8]); an important part of the evidence for a role for dimers originates from theoretical estimates of the fraction of water dimers among all water pairs at close to room temperature [30]. Thermodynamic considerations indicate that dimers (whose concentrations scale with the square of the partial pressure of water vapour) will be present at the Earth's surface with typically one-thousandth of the partial pressure of water vapour itself (e.g. [31,32]). The role of these dimers in explaining the continuum has been reinvigorated in recent years by the advent of theoretical quantum chemistry calculations which yield predictions of the strengths and positions of the dimer's rotational lines at far-infrared and millimetre wavelengths [33] and components of the dimer vibrational spectra (e.g. [34,35]) at visible and near-infrared wavelengths. This has enabled the identification and assignment of the partially-resolved rotational spectrum of water dimer lines in the microwave [36,37] and the relatively broad spectral features due to the dimer in near-IR water vapour bands at near-atmospheric conditions (e.g. [23,38–40]). It has also been proposed that particular spectral features can be explained by the fact that, in addition to bound (or stable) dimers, quasi-bound (or metastable) dimers should also be important in atmospheric conditions [6,36]. The quantitative analysis of these features, using a first-order approximation for the spectra of quasi-bound dimers, was found to be in reasonable agreement with theoretical calculations for the fraction of quasi-bound dimers made earlier in Refs. [30,41–43].

In the near infrared, theoretical calculations of dimer absorption do not yet account for rotation and for vibrational intermolecular modes in the dimer, which is required for the calculation of the absorption within the windows. Hence, while the continuum within the windows has been suggested to be plausibly due to the dimer (e.g. [6,44]), the attribution is inconclusive; the calculations are based on idealised assumptions about the width and shape of the dimer sub-bands, and, so far, on rather qualitative analysis of its temperature dependence. However, the quantitative analysis of temperature dependence performed earlier in the mid-IR window [45] demonstrated good agreement between the predicted and observed temperature dependence (see also [46]).

An alternative explanation of the water vapour continuum is that it is, at least partly, due to collision-induced absorption (CIA) (e.g. [5,47,48]), which results from interactions between pairs of molecules. Baranov and Lafferty [48] drew attention to the spectral similarity of CIA bands due to non-polar molecules (such as CO_2, N_2 and O_2) and the water vapour continuum, and asserted that dimer bands could not significantly contribute to continuum absorption far from their centres. This approach has been criticised in Ref. [6] and in more detail in Ref. [49], partly because there is no commonly accepted definition of the term CIA (especially for polar molecules like water), and in some cases CIA spectra include a significant dimer contribution [50,51]. It also remains essential to understand the quantitative contribution of different components of the bimolecular absorption to the observed continuum (some of which could be considered to contribute to CIA) such as free pairs and quasi-bound and true bound complexes. Until such understanding is in place, it appears difficult to establish a distinct role for CIA, relative to dimers.

3. Measurements of the water continuum in near-infrared windows

3.1. Overview of available measurements

Eight distinct windows can be identified in the infrared spectrum of water vapour, one centred on 1000 cm^{-1}, between the pure rotational lines of water vapour and the ν_2 vibrational band, and others between the successive vibrational bands, centred on about 2600, 4700, 6300, 8000, 9600, 11,500 and 13,000 cm^{-1} (see Fig. 1 for the structure to 10,000 cm^{-1}). We do not adopt a tight definition of where a window starts and ends, but each is typically a few hundred cm^{-1} wide.

The continuum in the 1000 cm^{-1} window has been extensively studied; uncertainties remain in both its strength and the temperature dependence (e.g. [14,46,52–54]) but these uncertainties are relatively small (around 10–15%) [54]. Although less studied, there is also a body of literature for the 2600 cm^{-1} window; most recent studies are in reasonable (within about 50%) agreement (see e.g. [6,16,23]). By contrast, laboratory measurements of the very weak water vapour continuum absorption in the 8000, 9600, 11,500 and 13,000 cm^{-1} windows are extremely sparse. Foreign and self continuum absorption measurements at the centre of the 8000 cm^{-1} window have been reported, mostly at elevated temperatures (i.e. 350–470 K) in the centre of the window [17,23] and at the edge of that window at room temperature [55], but we are not aware of any other laboratory measurements to compare these with. Fulghum and Tilleman [56] reported continuum absorption of $\alpha \sim 6 \times 10^{-10}$ cm^{-1} at 9466 cm^{-1} by calorimetric-interferometry for a 22 hPa partial pressure of water vapour in air with a total pressure of 1013 hPa. Table 1 reviews the available measurements in the 4700, 6300, 8000 and 9600 cm^{-1} windows. The corresponding techniques and experimental conditions of the measurements are indicated.

The focus here will be on the 4700 and 6300 cm^{-1} windows, where there is a growing set of measurements employing different techniques but where there are also significant disagreements. When appropriate, we also refer to the 2600 cm^{-1} window, as this is a useful benchmark given the greater number of measurements and better agreement, relative to the two windows discussed in detail here. There are 4 sets of measurements available, summarised in Table 1. These are:

(i) Fourier transform spectrometer (FTS) measurements as part of the UK CAVIAR (Continuum Absorption at Visible and Infrared wavelengths and its Atmospheric Relevance) project, which separates the self- and foreign-continuum contributions (see especially [17,23]).
(ii) Room-temperature FTS long-path measurements of the self-continuum [55,57] (henceforth "Tomsk" where the measurements were performed and analysed).
(iii) Laser methods, namely continuous-wave cavity ring down spectroscopy (CW-CRDS) and optical-feedback cavity enhanced absorption spectroscopy (OF-CEAS) [58–61] which were used to measure the self- and foreign continuum (henceforth "Grenoble" where the measurements were performed and analysed).
(iv) Bicknell et al. [62] using calorimetric-interferometry (CI), at room temperature (henceforth "Bicknell"); this study did not separately derive the self- and foreign-continuum components.

The measurement of weak broad-band absorption signals, which characterise the continuum in near-infrared windows, is particularly challenging. The different techniques used in these

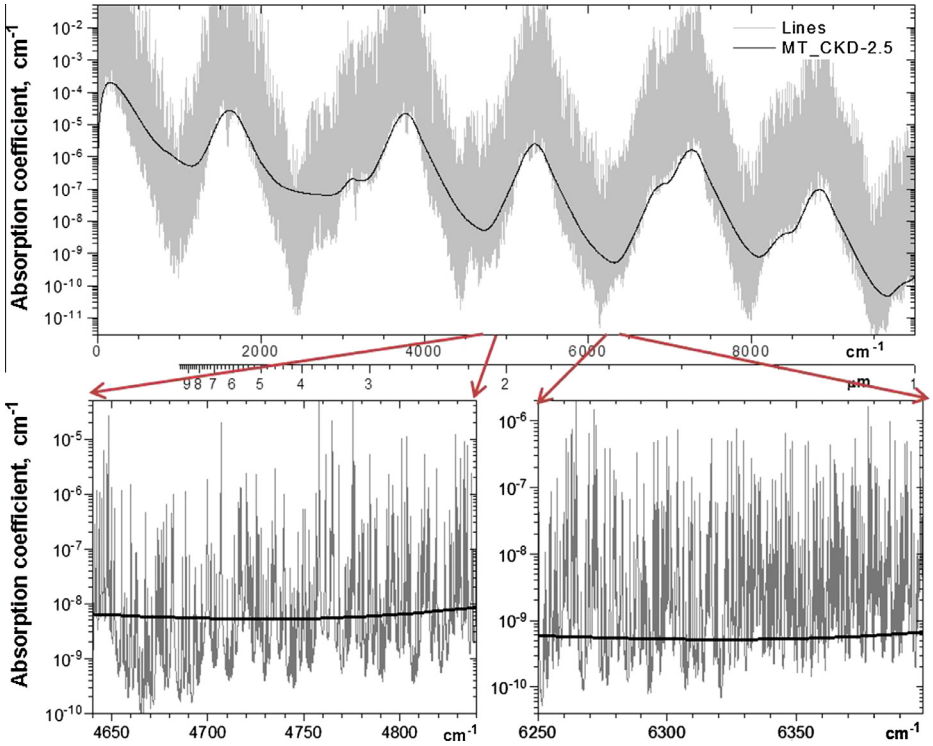

Fig. 1. Upper panel: High-resolution absorption spectra of water monomer lines and MT_CKD-2.5 continuum model [5] calculated for pure water vapour at pressure 13.3 hPa and 296 K. The water monomer spectrum (grey) is simulated using HITRAN-2012 [2] and a Voigt line profile with 25 cm^{-1} wings cut-off. The lower panels zoom into the centre of the 4700 cm^{-1} and 6300 cm^{-1} window to show the numerous microwindows (between lines) that can be used for retrieval of the continuum absorption from high-resolution experimental spectra.

Table 1
Summary of laboratory measurements of the water vapour continuum in four near-infrared windows. For the method, FTS is Fourier transform spectroscopy, CI is calorimetric interferometry, CRDS is cavity ringdown spectroscopy and OF-CEAS is optical-feedback cavity enhanced absorption spectroscopy. The parentheses in the temperature range column indicate that results are not presented for the entire wavenumber range, for the given temperatures.

Window	References	Method	Self/Foreign	Approx temperature range (K)	Approx. wavenumber range (cm^{-1})
9600 cm^{-1} (1.05 μm)	Ptashnik et al. [17,23]	FTS	S, F	(350) 431, 472	9100–9550
	Fulghum and Tilleman [56]	CI	S + F	303	9466
8000 cm^{-1} (1.25 μm)	Ptashnik et al. [17,23]	FTS	S, F	S: (350), 374–472 F: 350–431	7600–8550 8190–8600
6300 cm^{-1} (1.6 μm)	Bicknell et al. [62]	CI	S + F	298	6116–6160
	Ptashnik et al. [17,23]	FTS	S, F	S: (293, 350) 374–472 F: 350–431	S:5650–6650 F:5550–7020
	Ptashnik et al. [55,57]	FTS	S	289.5	5500–7050
	Mondelain et al. [60,61]	CRDS	S	296, 302–341	5875–6450 5875–6665
4700 cm^{-1} (2.1 μm)	Bicknell et al. [62]	CI	S + F	298	4590–4615
	Ptashnik et al. [17,23]	FTS	S, F	S: 293–472 F: 350–431	S: 3950–5150 F: 4020–5130
	Ptashnik et al. [55,57]	FTS	S	289.5, 318	3950–5150
	Mondelain et al. [59]	CRDS	S, F	297	4249, 4257
	Ventrillard et al. [58]	OF-CEAS	S	296–323	4302, 4723

studies have a variety of advantages and disadvantages. Except for the CI method, which is not an absolute absorption technique, the other techniques derive the continuum absorption by the difference of the light intensities transmitted through the absorption cell in the absence and in the presence of water vapour (and the foreign gas where appropriate). Consequently, the alignment of the spectrometer and the optical properties of the absorption cell must remain unaffected by the injection of water vapour. As discussed below, the resulting stability of the baseline during the cell filling and the entire measurement period is frequently the major error source.

The FTS method (as used in CAVIAR and Tomsk) has the advantage of being capable of measuring over a very broad wavenumber interval at high spectral resolution in a single measurement (2000–10,000 cm^{-1} at between 0.002 and 0.3 cm^{-1} spectral resolution in the case of CAVIAR). The baseline uncertainty, estimated in these experiments from the difference between background signals before and after the sample measurement, usually did not exceed 0.003–0.004 in optical depth, which for a total path length of ~1000 m in a long-path cell gives a sensitivity of about $3–4 \times 10^{-8}$ cm^{-1}. The detection of weak continuum signals normally requires the use of multi-pass absorption cells; these

can be heated to increase the available vapour pressure, although relative humidities well below 100% are employed to reduce the risk of droplet formation in the cell. The reported measurements are predominantly short-path (about 18 m) measurements with a temperature range 350–472 K (for CAVIAR), with some long-path (from 512 m for CAVIAR, to 612–1260 m for Tomsk) measurements at or near room temperature. To reduce the propagation of uncertainties in water vapour line-parameters (which must be removed to derive the continuum), the derivation is carried out within micro-windows between the lines. Hence, line parameter uncertainty only becomes significant towards the edges of the windows. As illustrated in Fig. 1, which compares the water vapour line-absorption with the MT-CKD2.5 continuum, even within the windows, there are many relatively strong lines which dominate over the continuum signal near their centre.

The principal source of experimental error when retrieving the continuum in windows using FTS lies in the baseline uncertainty (slow drifts) rather than the short-term signal-to-noise ratio of the instrument. Typically, sequential measurements are made, first with an empty cell, followed by one with a non-absorbing gas (such as argon), followed by a water sample measurement, followed again by non-absorbing gas and empty cell measurements (see e.g. [23] for details). Minimising instrumental drifts throughout this sequence is essential. (In addition, and as will be noted in Section 3.2, for some of the room-temperature FTS measurements, the whole FTS spectrum was adjusted to assumed values of the continuum strength in either higher or lower wavenumber windows.) Achieving a high signal-to-noise ratio is also beneficial since it allows a shortening of the measurement time, which may reduce the amplitude of drifts occurring between the sample and the non-absorbing gas and empty-cell measurements. In addition, the measurement procedure involves sample flushing, which is prone to produce mechanical variations in the cell's optics.

The relative uncertainty in the continua measurements obtained with the FTS (and with other techniques) generally decreases with increased sample temperature (as higher vapour pressures can be used at higher temperature, ensuring a higher signal). The relatively long measurement time required for the FTS technique means that it is important to monitor the stability of the temperature and pressure of samples within the absorption cell to guard, for example, against the loss of water molecules on to the surfaces in the cell. As an example, in the case of CAVIAR [17,23], measurements took up to 1 h, with pressure and temperature monitored at about 1 s intervals, and the variation in these parameters was included in the error estimates. With the FTS configurations and method of error estimation so far used, Ptashnik et al. [17,23] consider the FTS-retrieved continuum with $1-\sigma$ uncertainties of around 40–50% as "rather reliable", 20–30% as "rather good"; and below 20% as "good". The relative weakness of the continuum absorption in near-IR windows, and difficulties with the pure water vapour measurements, lead to the total uncertainties in the retrieved self-continuum from FTS being only rarely below 10%. In some spectral regions, the uncertainty in the FTS-retrieved continuum exceeds 50%, which is considered to provide some, at least, "semi-quantitative" information.

The CW-CRDS and OF-CEAS techniques used at Grenoble are both highly sensitive techniques based on the coupling of a laser with high finesse optical cavities. Both techniques offer a 4-decades dynamic range over an absolute, linear absorbance scale. CRDS and OF-CEAS exhibit a much higher sensitivity than FTS, but the measurements are limited to a few spectral intervals corresponding to the light frequency emitted by the available lasers. An advantage of these laser techniques is that they allow real-time monitoring of the absorption signal at a chosen wavelength, for instance during a pressure ramp.

A CRDS spectrum is obtained from the wavelength dependence of the lifetime of photons trapped in the cavity formed by two high reflectivity mirrors constituting the CRDS cell [63–65]. The absorption coefficient, $\alpha(\nu)$, at a wavenumber ν is determined from the measured cavity ring-down times, τ and τ_0, when the cell is filled and evacuated, respectively:

$$\alpha(\nu) = \frac{1}{c\tau(\nu)} - \frac{1}{c\tau_0(\nu)} \quad (2)$$

where c is the speed of light. The Grenoble CRDS set-up uses a 1.4 m long stainless steel CRDS cell wall with a 11.5 mm inner diameter. A record sensitivity of $\alpha_{min} \approx 5 \times 10^{-13}$ cm^{-1} level has been reported when measuring absorption lines [65]. CRDS measurements of the self-continuum were performed near 4250 cm^{-1} (2.35 μm) [59] and for fifteen selected wavenumbers between 5875 and 6450 cm^{-1} in the 6300 cm^{-1} window [60,61]. For 10.7 hPa of water vapour, the absorption coefficients were about 8×10^{-8} cm^{-1} at 4250 cm^{-1} and ranging between 1×10^{-9} and 8×10^{-9} cm^{-1} in the 6300 cm^{-1} window. By injecting argon or (dry) synthetic air, the baseline fluctuations were found to represent a few 10^{-10} cm^{-1} for CRDS and below 1×10^{-9} cm^{-1} for OF-CEAS experiments, corresponding to at most 1% and 10% of the measured absorption signals at 4250 cm^{-1} and in the 6300 cm^{-1} window, respectively.

Baranov et al. [54] reported a comparison of their FTS-derived continuum coefficients with CRDS-derived values from Cormier et al. [46]; at about 944 cm^{-1} and 310 K, they found the FTS values to be about 20% higher; this difference was outside the stated uncertainties of the two measurements. The fact that the CRDS measurements are lower than the FTS measurements in this window may be of some relevance to the FTS-CRDS comparisons presented in Section 3.2, but we note that the continuum in the near-infrared windows is typically 10–100 times weaker than in the 1000 cm^{-1} window and hence the experimental challenges are much greater.

The OF-CEAS technique [66] is an alternative to CRDS. It exploits optical feedback towards the diode-laser source occurring only at cavity resonances and allows optimised cavity injection by laser radiation. This is possible thanks to the adopted V-geometry of the high-finesse optical cavity. OF-CEAS generates repetitive spectral scans (several per second) in a small spectral region which contains few discrete absorption lines. Transmission spectra are obtained by dividing the cavity output signal by the reference laser power signal at each cavity-mode maximum. The inverse square root of this ratio is proportional to the cavity-loss rate with negligible error [67]. The proportionality factor is obtained by a ring-down measurement which is realised at the end of each laser scan [68]. Hence, OF-CEAS spectra are converted to cavity-loss spectra with an absolute absorption scale. While similar to CRDS, OF-CEAS allows a much faster profiling of a small spectral region; this is advantageous when measuring absorption continua as it yields information on the evolution of the spectral baseline together with the discrete absorption line profiles superposed on it, during rapid pressure ramps.

The Grenoble OF-CEAS continuum measurements were performed at 4302 and 4723 cm^{-1} using a V shape 493 mm long and 6 mm diameter cavity in a flow regime (while CRDS measurements were performed with static cells). The spectrum baseline was found to be affected by less than 10^{-9} cm^{-1} by the injection of air up to 27 hPa which represents about 2% compared to the smallest values measured with 21 hPa water vapour (about 5×10^{-8} cm^{-1} at 4723 cm^{-1}).

The CI technique used in Ref. [62] (and also in Ref. [56] in the study of the water vapour continuum absorption at 9466 cm^{-1}) is based on the interferometric detection of the optical path differ-

ence between two arms. More precisely, the CI absorption signal is obtained from the shift of the fringes induced by gas heating in one of the two arms of the interferometer where a (pulsed) excitation laser is co-aligned with the probe beam. As the same cell is inserted in the two arms of the interferometer, this approach should also be only weakly sensitive to the adsorbed water on the cell windows and to any kind of attenuation caused by scattering, which is not the case for FTS and laser absorption methods. However, the CI technique is not a direct measurement of absorption of radiation, and has to be calibrated using known absorption lines. Bicknell et al. [62] calibrated the continuum absorption at 1.63 and 2.17 μm using methane absorption at a different wavelength (2.2 μm). The calibration procedure supposes no change of the overlap geometry between the probe and excitation beams and of the shape of the pulsed excitation beam at the different wavelengths. While Fulghum and Tilleman [56] underlined the importance of monitoring the overlapping of the beam profile, Bicknell et al. [62] did not mention this issue, and thus it is not clear whether it was taken into account in the reported error bars. The method is nevertheless rather sensitive, allowing detection of absorption down to 10^{-10} cm^{-1} (e.g. [56]). We note that the Bicknell paper [62] is rather brief and does not give full details of the experimental set-up (for example, the exact vapour pressures used for measurements in the 6200 cm^{-1} window and how the baseline stability is assessed) nor does it examine the pressure dependence of the derived continuum; this has significantly limited our ability to analyse their results and compare with other work.

The continuum derived using these techniques are compared with MT_CKD Version 2.5 [5], because this continuum formulation is widely used (see Fig. 1). Within the two windows MT_CKD2.5 has not been constrained directly by measurements. Interestingly, the measurements of Ref. [62] (near 4600 cm^{-1} and 6140 cm^{-1}) and Ref. [56] (at 9466 cm^{-1}) mentioned above were used as part of the justification for applying a scaling factor that increased the strength of the 2600 cm^{-1} window self-continuum by up to a factor of 10, relative to earlier MT_CKD versions. These scaling factors strengthen the continuum relative to what is calculated using the line shape formulation in the 2600 cm^{-1} (see Section 2.2) window, but the unmodified line shape formulation is still used in Ref. [5] to derive the continuum strength in the 4700 and 6300 cm^{-1} windows. It is important to bear in mind, when comparing MT_CKD with observations, that MT_CKD does not report the uncertainty in their continuum. Other descriptions of the continuum are also available. The Tipping and Ma [69] far-wing theoretical model gives values of the continuum broadly similar to those in MT_CKD2.5 in the 4700 and 6300 cm^{-1} windows (see e.g. Fig. 3 of Ref. [9]). Paynter and Ramaswamy [70,71] have also produced a continuum model *via* a combination of MT_CKD2.5 and some of the measurements discussed in Sections 3.2 and 3.3.

3.2. Self-continuum

3.2.1. The 4700 cm^{-1} window

As shown in Table 1, all four groups (CAVIAR, Tomsk, Grenoble, Bicknell) have reported measurements in at least part of the 4700 cm^{-1} window. CAVIAR and Grenoble present information on the temperature dependence.

Bicknell's [62] CI measurements of the total continuum near 4600 cm^{-1} have been interpreted as being consistent with 6–12 times greater than the MT_CKD self-continuum [5] assuming that the self-continuum dominates; this assumption is itself subject to uncertainty (see Section 3.3).

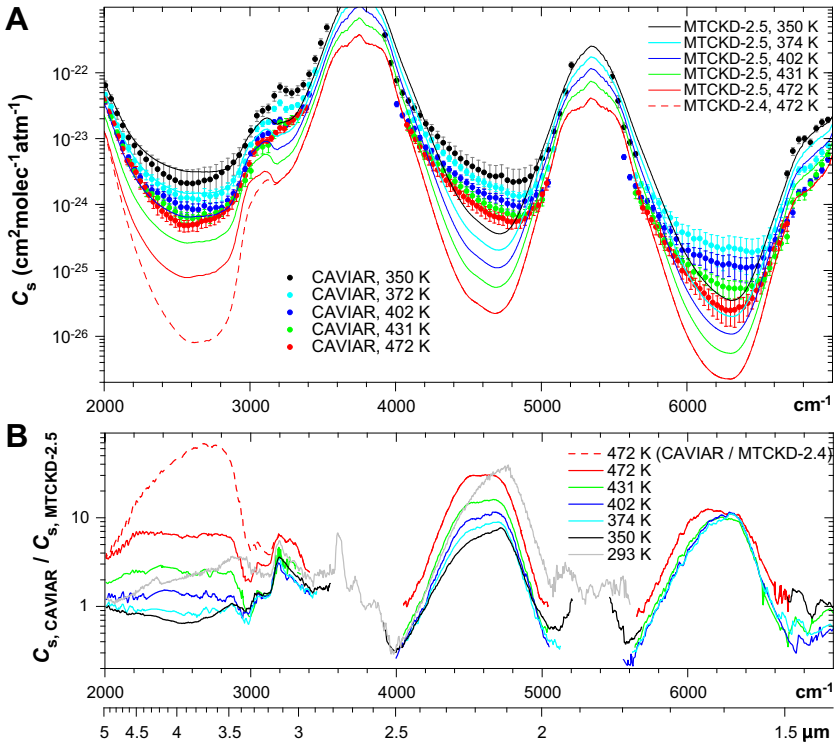

Fig. 2. (a) Absorption cross-section of the water vapour self-continuum, derived in (dots) from CAVIAR short-path cell measurements at temperatures between 350 and 472 K [23], compared to the MT_CKD continuum model [5] (note that MT_CKD-2.4 (dashed lines) and MT_CKD-2.5 (solid lines) are identical at wavenumbers greater than 3200 cm^{-1}). The error bars show experimental error (see text for details). (b) Ratio of the derived CAVIAR continuum (including long-path cell measurements at 293 K) to the MT_CKD-2.5 model at different temperatures; the ratio CAVIAR/MT_CKD-2.4 is also shown for the 2000–3000 cm^{-1} region. Redrawn from Ref. [23].

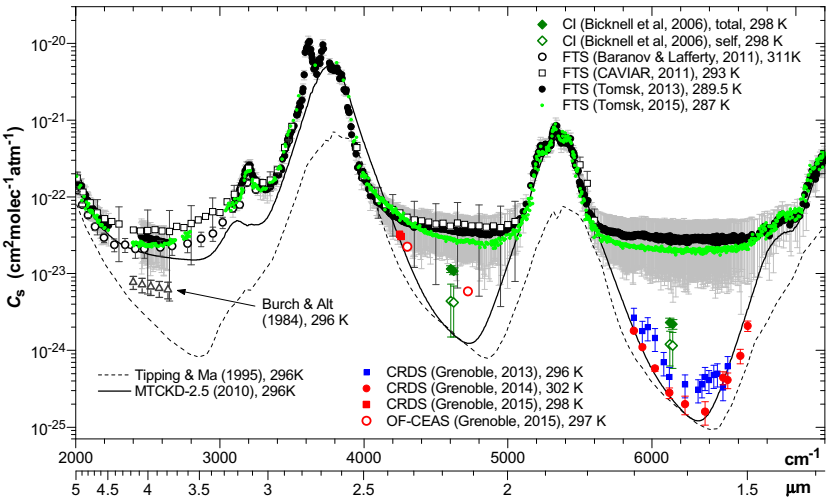

Fig. 3. Comparison of near-room temperature measurements of the water vapour self-continuum cross-sections between 2000 and 7000 cm^{-1}. The Bicknell et al. [62] self-continuum cross-sections were estimated here by subtracting from the total continuum absorption derived in that work the contribution of the foreign continuum using the high-temperature CAVIAR experiments [17], assuming very weak *T*-dependence of the foreign continuum. The reported error-bars of the Grenoble 2015 data lie within the symbol size. Also shown are the self-continuum from the MT_CKD2.5 [5] and Tipping and Ma [69] models.

As illustrated in Fig. 2, in the centre of the window (approx. 4400–4800 cm^{-1}), CAVIAR short-path FTS self-continuum cross-sections [23] are systematically higher than MT_CKD2.5 by between factors of 6 at 350 K, and a factor of 30 at 472 K; these differences exceed measurement uncertainty by an order of magnitude. Long-path measurements at 293 K are also stronger than MT_CKD2.5 by up to a factor of 30, but with much lower confidence (Fig. 3). Towards the edge of the window between 350 and 431 K, CAVIAR is lower than MT_CKD2.5 by typically a factor of 2. Many of the short-path measurements at temperatures greater than 350 K were repeated at several vapour pressures and the measured optical depth was shown to vary as the square of the vapour pressure [23] within the uncertainty of the measurements, as expected for the self-continuum (see Section 2.1).

The Tomsk FTS long-path measurements [55] were performed at 290 and 318 K. In this set of measurements, the baseline stability was assessed by comparing empty and full cell measurements; the baseline stability at around 9300 cm^{-1} was monitored and shown to be reliable, such that the signal at that wavenumber needed to be adjusted, on average, by less than 0.5% to ensure empty and full cell signals were equal; without this adjustment, the derived cross-sections would be higher. This assumes that the continuum is negligible at 9300 cm^{-1} for such measurement conditions. While little information is available to fully justify this, Fulghum and Tilleman's [56] near-room temperature measurement of the self- plus foreign-continuum at 9466 cm^{-1} was about 5×10^{-26} cm^2 molec^{-1} atm^{-1}, about a factor of 2 greater than MT_CKD2.5 at this wavenumber. Assuming the 9300 cm^{-1} value is an order of magnitude stronger than this (as it is nearer the edge of the window than the measurement of [56]), it would still be about a factor of 100 weaker than the Tomsk-derived continuum at 4700 cm^{-1}. It is noteworthy that the Tomsk FTS results indicate that while the room-temperature self-continuum is roughly constant between the centres of the 2500, 4700 and 6300 cm^{-1} windows (Fig. 3 – the 6300 cm^{-1} window will be discussed in Section 3.2.2), it would need to fall by two-to-three orders of magnitude by 9600 cm^{-1} to be consistent with the implied weak continuum in the 9300 cm^{-1} window.

The Tomsk 290 K results are in reasonable agreement with CAVIAR 293 K results (within 30–40%, accounting for the slightly different measurement temperatures) (Fig. 3), and well within the measurement uncertainties. The Tomsk relative uncertainties are a factor of 2 lower than CAVIAR, because of better baseline stability and longer path length.

Ptashnik et al. [57] reported a repeat of the Tomsk FTS measurements at 287 K using a longer optical path-length and new mirrors (see Fig. 3); the new results are a factor of ≈1.5 lower than [55] due mostly to a different choice of baseline adjustment; the absolute level of the measurements was adjusted to be the same as MT_CKD2.5 at 287 K in the 2500 cm^{-1} window where most recent assessments are in reasonable agreement (see Fig. 3). MT_CKD2.5 was chosen as it is the lowest of the more recent estimates of the strength of the continuum in the 2500 cm^{-1} window and so can be considered a "conservative" choice. Therefore, the main aim of measurements in [57] was to derive the relative values of the strength of the self-continuum absorption, in near-IR windows relative to MT_CKD2.5 at 2500 cm^{-1}.

The high-sensitivity CRDS [59] and OF-CEAS [58] self-continuum measurements were made at 4 wavenumbers towards

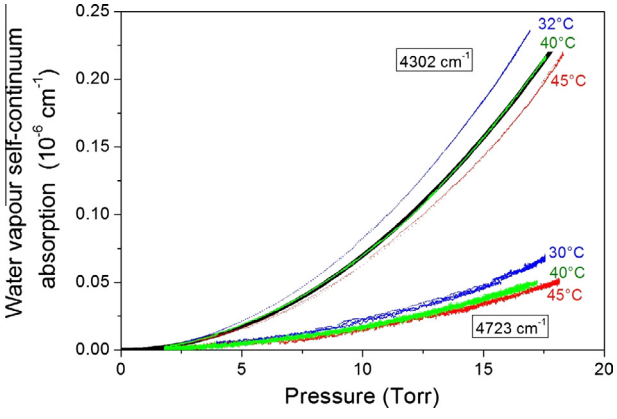

Fig. 4. Pressure dependence of the water vapour self-continuum absorption at 4302 and 4723 cm^{-1} for temperatures from 303 to 318 K from OF-CEAS measurements (coloured lines) [58]. At 4302 cm^{-1} and 40 °C, the black curve shows the quadratic fit to the measurements and demonstrates the quadratic dependence of absorption with vapour pressure. At 4723 cm^{-1} there is a higher noise level which is due to lower mirror reflectivity; the multiple lines at 4723 cm^{-1} are derived from several pressure cycles, and illustrate the measurement repeatability (adapted from Ref. [58]). (For interpretation of the references to colour in this figure legend, the reader is referred to the web version of this article.)

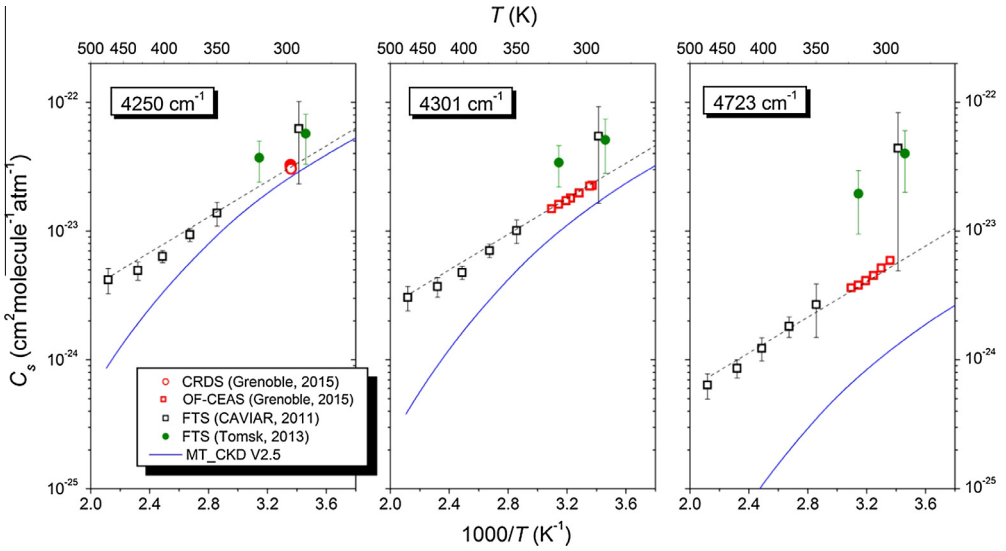

Fig. 5. Temperature dependence of the water vapour self-continuum cross-section at three wavenumbers in the 4700 cm^{-1} window (after [58]) from Grenoble CRDS (open red circles), OF-CEAS (open red squares), CAVIAR FTS (open black squares) and Tomsk FTS (filled green circles), and the MT_CKD2.5 continuum model. The dashed lines show the slope of the curve assuming a temperature dependence of the form exp (D/kT) with D_o = 1104 cm^{-1} (see text for details). (For interpretation of the references to colour in this figure legend, the reader is referred to the web version of this article.)

the edge (4249, 4257 and 4302 cm^{-1}) and near the centre (4723 cm^{-1}) of this window. The measurements were made at room temperature; the OF-CEAS measurements at 4302 and 4723 cm^{-1} were also performed at 5 further temperatures up to 323 K. Fig. 4 shows the variation of the derived continuum absorption with vapour pressure, which presents compelling evidence of the purely quadratic dependence. The OF-CEAS self-continuum cross-sections, C_S, were derived from the quadratic fit of α_v versus P^2. The statistical errors of the fit are negligible (<0.1%) and the uncertainty budget led to 3% and 5% total error bars for the C_S values at 4302 and 4723 cm^{-1}, respectively.

The room temperature Grenoble self-continuum cross-sections are included in Fig. 3. By contrast with the CAVIAR/Tomsk FTS C_S values, at the centre of the window, the measurements are within a factor of 5 of MT-CKD2.5, and hence much closer to MT_CKD2.5 than the room-temperature FTS measurements. This offset is roughly constant with temperature, across the 296–323 K temperature range of the OF-CEAS measurements (Fig. 5). While not formally outside the uncertainty estimates of the CAVIAR room-temperature values, the Grenoble data are outside those derived for the Tomsk measurements. Although not at the same wavenumber as the Bicknell CI measurements, and noting the difficulties in separating out the self- and foreign-continuum components of those measurements, the OF-CEAS measurements are consistent with Bicknell in this window. Away from the centre of the window, the CRDS and OF-CEAS measurements near 4250 cm^{-1} are 20–40% higher than MT_CKD2.5, and lie within the uncertainties of the Tomsk FTS measurements.

As discussed in detail in Ref. [58], taken together the CRDS/OF-CEAS measurements and the short-path CAVIAR measurements at 350 K and above agree with a simple exp (D/kT) temperature dependence where the derived D is also quite consistent with the dissociation energy ($D_0 \sim 1105$ cm^{-1}) of the bound water dimer (Fig. 5).

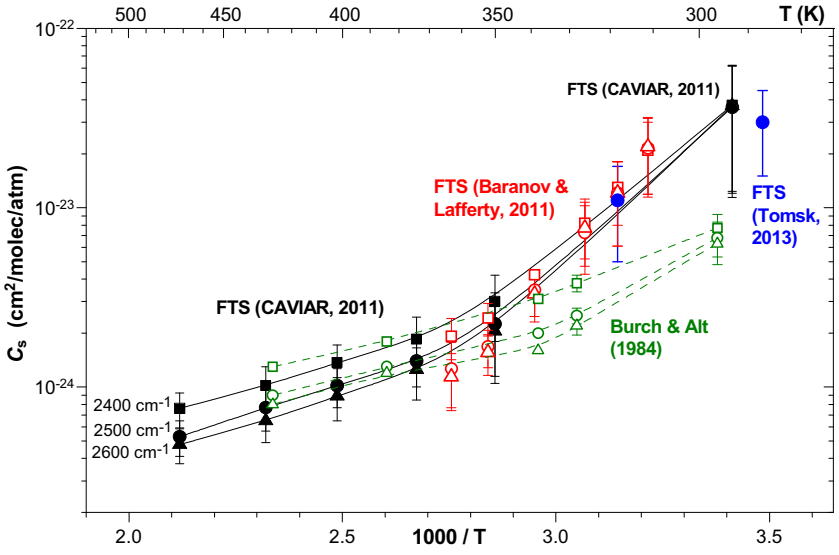

Fig. 6. Temperature dependence of the water vapour self-continuum cross-sections in the middle of the 2500 cm^{-1} window from three different FTS measurements (CAVIAR [23], Baranov and Lafferty [16] and Tomsk [55]) and from Burch and Alt's [14] grating-spectrometer measurements. All measurements used multi-pass cells.

However, as pointed out in Ref. [58], the interpretation of this agreement is not straightforward and should be treated with caution. Based on a simple model, Vigasin [45] suggested the temperature dependence of the dimer absorption cross-section is proportional to $T^{2-n}\exp(D_0/kT)$, where n is a parameter related to the number of rotational and vibrational degrees of freedom in the dimer, which can itself be a function of temperature. As shown by Ref. [45], $n = 1.63$ (which is close to the harmonic oscillator approximation where $n = 1.5$) agrees reasonably well with the observed temperature dependence of the self-continuum in the microwave and in the mid-infrared window at close to room temperature (see also [46]). But it is less clear if it is applicable in the near-infrared (see also Section 3.2.2). The temperature dependence of the self-continuum in the neighbouring 2500 cm^{-1} window does not support a simple exp (D/kT) extrapolation (Fig. 6). FTS measurements by CAVIAR [23] and Baranov and Lafferty [16], covering 290–450 K, show a significant change in the log-scaled slope. By contrast, the older Burch and Alt [14] results (Fig. 6) show a less marked temperature dependence; however, below 350 K, these measurements do not agree with any of the 3 more recent FTS studies, nor with MT_CKD2.5. A possible qualitative explanation of the different temperature dependences was suggested by Pavlyuchko and Vigasin [72] (see also [6]). They suggested that the transition between stable and quasi-bound dimers as the dominant contributors to the dimer population could lead to a deviation from the pure exponential form; such a transition should occur close to room temperature [41,42]. This reasoning was used in Ref. [6] to tentatively attribute the stronger T-dependence at near-room temperature in the near-infrared windows to this transition.

One feature of note in comparing the continuum strength in the 2500 cm^{-1} and 4700 cm^{-1} windows (see Fig. 3) is that in all the CAVIAR and Tomsk FTS measurements, the minimum in the 4700 cm^{-1} window is as high, if not higher, than the minimum in the 2500 cm^{-1} window. There is much more confidence in this conclusion in the higher-temperature CAVIAR measurements (Fig. 2), where the uncertainties are much smaller than at room temperature (Fig. 3). Much earlier high-temperature (575 K and above) measurements using a grating interferometer by Hartmann et al. [73] (the values are presented in Ref. [23] in the continuum units used in this paper), suggest the same behaviour although they do not reach the wavenumbers of the minimum in the 4700 cm^{-1} window. Figs. 2 and 3 show the same feature in the theoretical Tipping and Ma [69] model and in MT-CKD2.4. (It is not appropriate to compare the relative strength of MT-CKD2.5 in these two windows; as discussed in Section 3.1, Ref. [5] noted the likely need to adjust the strengths in both windows, but for MT-CKD2.5 they only did so for the 2500 cm^{-1} window.) If this similarity in continuum strength in these two windows is a robust feature, then there is an important corollary. The room-temperature OF-CEAS and Bicknell measurements in the 4700 cm^{-1} are much lower than the recent FTS measurements (and MT-CKD2.5) in the 2500 cm^{-1}; this may be evidence that the continuum strength in the 2500 cm^{-1} window in FTS measurements and MT-CKD2.5 is itself overestimated by around a factor of 5. This emphasises the need for different techniques to be applied in all relevant window regions. It is also important to test whether the relative strengths of the continuum in neighbouring windows, as derived by FTS measurements, are robust over the full temperature range.

3.2.2. The 6300 cm^{-1} window

The four experimental groups have also reported measurements in at least part of the 6300 cm^{-1} window (Table 1). CAVIAR and Grenoble present information on the temperature dependence. Bicknell's room temperature CI measurement of the self- plus foreign-continuum near 6150 cm^{-1} were found to be typically 9 times stronger than MT_CKD [62]; the self-continuum itself would be about factor of 5 stronger if the CAVIAR estimate of the foreign continuum (see Section 3.3) is removed from the total continuum, noting the considerable uncertainty in this correction.

The CAVIAR FTS continuum retrievals (Fig. 2) were only possible at temperatures above 374 K in the core of the window, with some measurements at 293 K and 350 K at the edges of the window where the continuum was stronger. In the core of the window, as in the 4700 cm^{-1} window, CAVIAR is considerably stronger than MT_CKD2.5, by about an order of magnitude, while towards the edge of the window, this ratio falls until CAVIAR is weaker than MT_CKD2.5 by about a factor of 2. One notable (and unexplained) feature, compared to the 4700 cm^{-1} window, is that the CAVIAR/MT_CKD ratio is much more constant with temperature, and essentially identical between 374 and 431 K (see Fig. 2b). Since the MT_CKD temperature dependence is identical in all windows, this strongly suggests that the temperature dependence of the continuum varies significantly from window to window. This feature would have to be explained in any comprehensive theoretical description of the continuum.

The Tomsk FTS measurements [55] (Fig. 3) found an unexpectedly strong room-temperature self-continuum, more than a factor of 100 greater than MT_CKD2.5 in the centre of the window, and so quite different in this respect to the higher-temperature CAVIAR measurements (Fig. 2). The uncertainty in the centre of the window is large, exceeding 50% of the central estimate, so that the measured absorption signals exceeds the baseline uncertainty by less than a factor of 2. However, even if the derived continuum is at the lower end of this 1-σ uncertainty range, it would still be much stronger than MT_CKD2.5. Towards the edges of the window (near 5600 cm^{-1}), CAVIAR and Tomsk agree, within their respective uncertainties, and agree with MT_CKD2.5. Ptashnik et al. [55] explored possible reasons that may have an overestimate in the centre of this window; this included the influence of engine oil contamination (from the vacuum pumps) in the cell, and the formation of droplets and adsorption of water vapour on the mirrors, but none provided a compelling explanation.

As in the 4700 cm^{-1} window, the continuum strength derived in Ref. [57] (see Section 3.2.1) in this window, are a factor of $\approx$1.5 lower than in Ref. [55] (Fig. 3). Nevertheless they remain much stronger than other analyses. The possibility of some unidentified absorption or baseline shift in the large-cell FTS measurements still cannot be excluded. Given the degree of agreement between the CAVIAR and Tomsk FTS measurements in the 4700 cm^{-1} and 2500 cm^{-1} windows (Fig. 3), however, that absorption (or baseline deviation) would have to manifest itself in the same way in both FTS systems. Such a similar baseline deviation is considered rather unlikely.

Mondelain et al. [60,61] measured the continuum at 10 wavenumbers in the 6300 cm^{-1} window using the Grenoble CRDS set-up. We will focus on Ref. [60]; the results are felt to be more reliable and also include temperature dependence. Their results (Fig. 3), and the CAVIAR FTS high-temperature measurements (Fig. 2), show the continuum in the centre of this window to be more than a factor of 10 weaker than in the 4700 cm^{-1} window; by contrast, in the room temperature Tomsk FTS measurements, the continuum strength is significantly stronger, and of approximately the same strength at the centre of the two windows (Fig. 3). For the weaker continuum in the 6300 cm^{-1} window (corresponding to an absorption coefficient of 10^{-9} cm^{-1} for a 13 hPa water pressure), the pressure dependence was not found to be purely quadratic as was the case at 4300 cm^{-1} (Fig. 4), but included a linear dependence in vapour pressure. Mondelain et al. [60] interpreted this linear term contribution to be due to adsorption of

water on the mirrors in the cell; the quadratic term was used to derive the self-continuum cross section. At the centre of the window, and at higher vapour pressures, about 30% of the observed extinction was attributed to the condensate and then subtracted from the measured signal. Mondelain et al. [60] noted that for the weaker continuum in this window there was also a possible contribution of systematic error in these experiments related to the absorbate that was not fully quantified. This systematic error was estimated to be no more than 10% at the centre of the window.

Mondelain et al. [60] found the near-room-temperature (302 K) continuum to be about 60 times weaker (after accounting for temperature dependence) than that found by Ref. [55] near the centre of the window, and about 10 times weaker at the lowest wavenumber measured by CRDS (see Fig. 3). It was also factor of 5 weaker than the self-continuum estimated by Ref. [62] (again, noting the uncertainty in this estimate). At 302 K, the measurements agree with MT_CKD2.5 within about 50%.

The temperature dependence found in the CRDS measurements is weaker than the CAVIAR FTS measurements at higher temperatures (see Fig. 7), and weaker than the observed dependence in the 2500 and 4700 cm^{-1} windows (Figs. 5 and 6). This is most marked near the centre of the window (Fig. 7b). And while the CRDS results agree with MT_CKD2.5 within 50% at 302 K, they disagree by a factor of 3 at 340 K. At 6121 cm^{-1} (Fig. 7), within the measurement uncertainties, the simple temperature extrapolation of the higher-temperature CAVIAR measurements is broadly consistent with the Bicknell CI measurement, which includes the self- and foreign continuum contributions.

Fig. 7 shows that the room-temperature Tomsk measurements appear strongly inconsistent with all other measurements; to reconcile these, it would require a very strong upward curvature of the temperature dependence, relative to the higher-temperature measurements.

3.3. Foreign continuum in the 4700 and 6300 cm^{-1} windows

The only published broadband foreign-continuum measurements in these windows are the CAVIAR FTS measurements [17] for temperatures of 350–430 K. Mondelain et al. [59] report the CRDS-derived foreign continuum at 4250 cm^{-1} at 298 K. Both used dry synthetic air relevant to the atmosphere. The CRDS C_F value was derived from a linear fit of the absorption signal for air pressures up to 1000 hPa (see Eq. (1)). The foreign-continuum derived from laboratory measurements is the difference between the total measured continuum and the self-continuum, and hence uncertainties in the self-continuum impact the derived foreign-continuum. The foreign continuum appears approximately independent of temperature, within experimental uncertainty, both

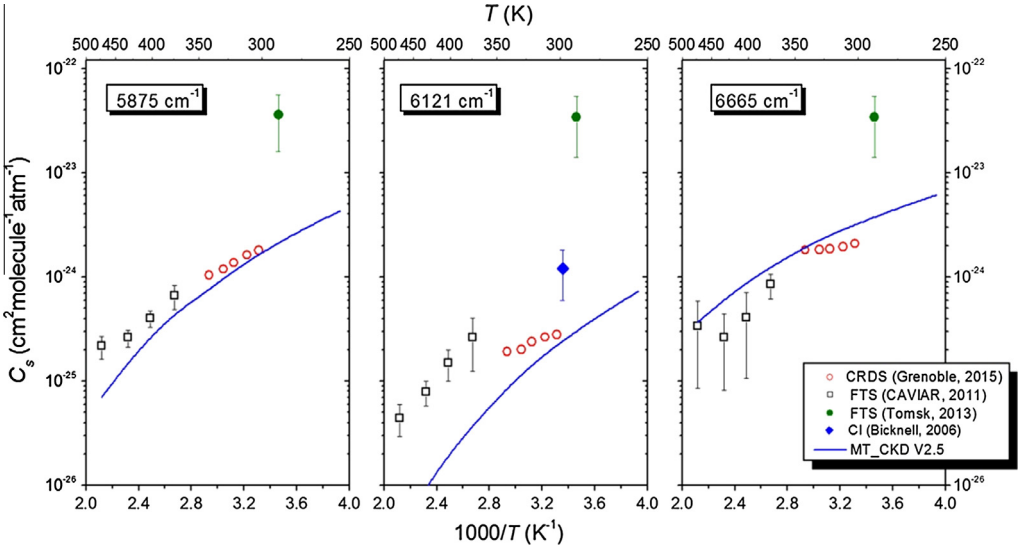

Fig. 7. Temperature dependence of the water self-continuum cross sections, C_S, from Grenoble CRDS [60], CAVIAR FTS [23], from Tomsk FTS [55] and Bicknell et al. CI [62] near the low energy edge (5875 cm^{-1}), near the centre (6121 cm^{-1}) and near the high energy edge (6665 cm^{-1}) of the 6300 cm^{-1} window. Bicknell et al. reported only the sum of the self and foreign continua with a 30% error bar.

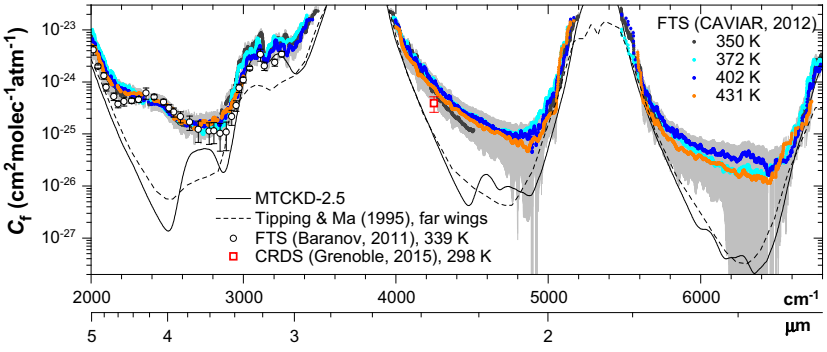

Fig. 8. (a) Water vapour foreign continuum cross-section derived from CAVIAR FTS measurements (H_2O–Air) at 350, 372, 402 and 431 K [17], experimental data of FTS measurements (H_2O–N_2) in 2500 cm^{-1} window [75] and CRDS measurements (H_2O–Air) at 4250 cm^{-1} [59]. The foreign continuum models MT_CKD-2.5 [5] and Tipping and Ma [69] are shown for comparison. The shaded areas show the estimated total error of the CAVIAR continuum.

in these windows and in lower wavenumber windows [74,75]; this is an advantage as measurements at high vapour pressure (and hence temperature) remain relevant to the atmosphere.

Fig. 8 shows the derived foreign continuum values from CAVIAR and Grenoble. The FTS uncertainties vary from around 10% at the edges of the windows where the continuum is strongest, to approaching 100% in the weaker parts, most notably between 6200 and 6500 cm^{-1}. At 4250 cm^{-1}, CAVIAR and Grenoble are in reasonable agreement, with CAVIAR 1.7 times higher than Grenoble, with overlap between their uncertainty estimates (about 30% for both). By contrast both measurements are considerably stronger than MT_CKD2.5 – away from the very edges of the windows, the central estimates from CAVIAR are 5–100 times stronger, while the Grenoble value is 5 times higher (and closer to the CAVIAR value at the measured wavenumber).

Other supporting evidence for a much increased foreign continuum values comes from the degree of agreement between CAVIAR and the FTS measurements (with nitrogen, rather than air as the broadening gas) of [75] in the neighbouring 2500 cm^{-1} window (Fig. 8). The observed foreign continuum does not solely involve water molecules. Although the strong N_2–N_2 collision-induced absorption band in this region has been removed from the observed continuum [17], the component of the nitrogen (or oxygen) absorption involving interaction with water molecules still gives the dominant contribution to foreign continuum absorption in this spectral region. Disagreement between the CAVIAR and Baranov values does not exceed 30–50% which lies within experimental uncertainty, and at 2500 cm^{-1} both are stronger than MT_CKD2.5 by a factor of more than 100. Although at the core of the 4700 cm^{-1} window (between about 4600 and 5000 cm^{-1}) the retrieved foreign-continuum is weaker than the continuum in the 2500 cm^{-1} window, it is of comparable strength, and with comparable uncertainties, to the 2500 cm^{-1} continuum, at wavenumbers less than 4600 cm^{-1}.

3.4. Synthesis

The available measurements of the self-continuum in the 4700 and 6300 cm^{-1} windows do not provide a picture which is consistent across all measurements and across both the windows which are the focus here. There is a strong indication that the MT_CKD2.5 continuum is generally too weak towards the centre of the 4700 cm^{-1} window, which is essentially acknowledged by [5], but the degree by which it is too weak differs significantly amongst measurements and between temperatures. There is less consensus in the 6300 cm^{-1}, where the Grenoble laser measurements roughly agree with MT-CKD2.5 near room temperature.

In the 4700 cm^{-1} window, the higher-temperature CAVIAR measurements and the lower temperature Grenoble measurements are consistent with a simple exponential law in $1/T$ over the 296–472 K temperature range. This is also the case at the edge of the 6300 cm^{-1} window, but is not the case near the centre of that window. The CAVIAR FTS results (see Fig. 9 in Ref. [23] and Figs. 5 and 7 here) indicate that between temperatures of 374 and 472 K, the slope of the temperature dependence at the centre of the 6300 cm^{-1} window is about twice that found at the centre of the 4700 cm^{-1} window. By contrast, in the Grenoble measurements, the temperature dependence (over the approximate range 300–330 K) in the centre of these two windows also differs by around a factor of 2, but it is now the 4700 cm^{-1} window which has the stronger dependence (see Figs. 5 and 7). Although the actual form of the temperature dependence remains unclear, the available evidence indicates that the temperature dependence in these two windows does indeed differ. Further, the recent FTS measurements in the 2500 cm^{-1} window (Fig. 6) indicate that the assumption of the simple exponential law in $1/T$ does not hold in that window across the range 293–472 K.

The Tomsk 297 K and 317 K measurements are outliers compared to other measurements. However, we note that although uncertainties are large, there is a good agreement between the Tomsk and CAVIAR room temperature cross-sections in the centre of the 4700 cm^{-1} and consistency with the more confident measurements of CAVIAR and other recent measurements in the 2500 cm^{-1} window (Fig. 3). As noted in Section 3.2.1, it is important to assess whether this consistency is a reliable indicator. In addition, the use of alternative assumptions about temperature dependence, rather than the simple exponential law in $1/T$, could make the room temperature measurements more consistent with the high-temperature CAVIAR measurements. However, it is much harder to use a similar argument in the centre of the 6300 cm^{-1} window, where the Tomsk FTS and Grenoble CRDS measurements differ by a factor 60 (compared to a factor of 5.5 in the 4700 cm^{-1} window) near room temperature (Fig. 7). The near-constancy of the room temperature continuum across the 2500 cm^{-1}, 4700 cm^{-1} and 6300 cm^{-1} windows in the Tomsk FTS results is at variance with that found in the CRDS/OF-CEAS results in the 4700 and 6300 cm^{-1} windows. In addition, the 2013 Tomsk FTS [55] results were derived on the basis that the continuum at 9300 cm^{-1} was considered to be negligible. Hence these results would require a rapid decrease in continuum strength between the 6300 cm^{-1} and 9600 cm^{-1} windows to be consistent; further measurements in these higher wavenumber windows are needed. The C_S values reported by CRDS in the centre of the 6300 cm^{-1} window correspond to an absorption coefficient at the level of a few 10^{-9} cm^{-1} for a 13 hPa pressure. The absorption losses at the 10^{-7} cm^{-1} level measured by the Tomsk FTS are incompatible with the CRDS observations.

There is no doubt that the inherent sensitivity of laser methods is superior in measuring weak continuum absorption in the windows, and should be favoured. In addition, laser methods allow the retrieval of cross sections by fitting the pressure dependence of the observed absorption. In the 4700 cm^{-1} window, the CRDS and OF-CEAS pressure dependence was observed to be purely quadratic for the self-continuum and purely linear for the foreign continuum. In the 6300 cm^{-1} window, where the continuum is much weaker than in the 4700 cm^{-1} window, the pressure dependence of the self-continuum included a linear term which was interpreted to be due to water adsorbed on the CRDS mirrors. This is the reason why the CRDS C_S error bars, which are on the order of a few % at 4700 cm^{-1}, are larger and more difficult to estimate at 6300 cm^{-1}. By contrast, the pressure dependence of the absorption signal in the 4700 and 6300 cm^{-1} windows has not yet been investigated using FTS for near room-temperature conditions – instead the continuum was derived from measurements made at a single pressure. An investigation of the pressure dependence would provide important evidence as to whether the room-temperature FTS data is related to a bimolecular water vapour self-continuum (as it is currently interpreted to be), or whether it has some other physical, or instrumental, origin.

Thus, it is possible that the room-temperature FTS measurements were affected by some unrecognized absorption or attenuation in the large FTS cells, which leads to the 4700 cm^{-1} and 6300 cm^{-1} measurements being overestimated. If the 4700 cm^{-1} self-continuum in room temperature FTS measurements is an overestimate and if (as discussed in Section 3.2.1) the continuum in the 4700 cm^{-1} and 2500 cm^{-1} windows are of similar strength, then the self-continuum derived from recent FTS measurements in the 2500 cm^{-1} window may also be too strong.

Hence there are clear puzzles to be resolved and few measurements with which to compare them (including completely independent FTS/cavity estimates made and analysed in different laboratories). As well as differences in the spectroscopic techniques,

there is also a significant difference in the absorption cells, which may play some role. CRDS and OF-CEAS cells are characterised by being rather narrow (about 10 mm diameter) and have a much larger surface-to-volume ratio than for typical FTS absorption cells (diameters of tens of centimetres). Ventrillard et al. [58] briefly discuss this issue in the context of their 4700 cm^{-1} measurements, and conclude that surface effects do not likely play a role. This seems to be supported by the consistency of the CRDS/OF-CEAS results with the higher temperature CAVIAR FTS measurements performed with a large cell, assuming the simple form of the temperature dependence is correct. Nevertheless it would be reassuring to show that the observed continuum strength is indeed independent of the cell size in both FTS and CRDS/OF-CEAS systems.

4. Conclusions and possible future directions

From the discussion in Section 3, two main points emerge. The first is the scarcity of laboratory measurements of the near-infrared water vapour continuum, in conditions close to those relevant to the atmosphere. For the two window regions which are the focus here, and for the self-continuum, only one group has reported cavity-enhanced absorption measurements, at a few selected wavenumbers, and only two groups have reported FTS measurements and, even then, the measurements were analysed using a common method. The situation for the foreign continuum is even sparser, with only one set of FTS measurements and a single wavenumber derivation using CRDS. One group has (rather briefly) reported CI measurements of the total ($H_2O + N_2$) continuum in very narrow spectral intervals.

While there are some mutually supporting aspects of these analyses, the measured continuum strength in the centres of the 4700 cm^{-1} and 6100 cm^{-1} windows at room temperature are in profound (around an order of magnitude) disagreement. There is, as yet, no compelling explanation for these differences; nevertheless the inherent precision of the cavity-enhanced laser techniques would naturally favour their results. The difference is important from an atmospheric perspective. If self-continuum absorption is broadly at the level of MT_CKD2.5, the water vapour self-continuum absorption in near-infrared windows would be of limited importance for atmospheric energy budget calculations and analyses of satellite data (although the strengthened foreign continuum (relative to MT_CKD2.5) could still play a role). By contrast, if the continuum were as strong as indicated in the room-temperature FTS measurements, it would significantly influence both these perspectives. The calculated atmospheric absorption of solar radiation would increase [17,76], as would the "interference" by water vapour for remote sensing of cloud or other parameters [9]. Hence it is important that the reasons for the differences be understood and several routes are needed. The existing methodologies can be improved in many ways to boost the accuracy and the wavelength range of the measurements (see below).

The second point is that even measurements at near-room temperature (290–295 K) are hardly representative of the atmosphere – for example, on a zonal (i.e. averaged over all longitudes) and annual mean, the temperature is greater than 290 K only within about 40° of the equator and below about 2 km in height. One key result from current measurements is the apparent variation in the temperature dependence of the self-continuum both with temperature itself, and between windows; hence, the simple extrapolation of existing measurements to lower temperatures is unlikely to be reliable. There is a need to expand the parameter space of laboratory measurements to cover conditions more representative of the atmosphere.

In our opinion, a robust observationally-based water-vapour continuum across broad spectral regions cannot yet be recommended for inclusion on spectroscopic databases such as GEISA and HITRAN. We discuss here how possible technical developments could provide a path for such an inclusion in the future. We stress that there would be a very clear benefit if more measurements and independent analyses were available from other laboratories, even using existing techniques.

4.1. Fourier transform spectroscopy

The main source of uncertainty in FTS continuum measurements is baseline stability. The priority is to reduce low frequency noise (drifts). The reduction of single spectral point noise would also be beneficial as it would yield higher signal-to-noise ratio (SNR) and relax the baseline stability time requirements, allowing faster measurements for a given SNR. A number of developments of FTS could improve SNRs which would decrease uncertainties, and also allow the temperature range at which continuum measurements are made to be expanded.

One approach is to move away from traditional halogen tungsten lamps as broadband sources for FTS. For example, supercontinuum light sources (SCLS) are a recent compact way of generating "white" light over a relatively wide continuous band (e.g. [77]). SCLS exploits several non-linear effects which occur while a femto-second laser pulse propagates within a photonic crystal fibre. SCLS are particularly well developed and commercially available in the visible/near-infrared part of the spectrum (0.4–2 μm) and are beginning to expand deeper into the infrared. Compared to traditional lamps, SCLS can be several orders of magnitude brighter, and their spatial coherence can be further exploited to increase the path length through higher gain absorption cells that are not suited for incoherent light. For instance, Herriott and Schulte [78] and even astigmatic multipass cells [79] could yield a significant (up to ~10 times) increase in path length for a given sample volume. Alternatively, using SCLS combined with cavity-enhanced FTS schemes [80] could bring several orders of magnitude improvement in measurement precision.

We report here results from a recent pilot experiment at the Rutherford-Appleton Laboratory (RAL), UK, to examine the potential for coupling SCLS sources (in this case a Fianium SC 400 and a NKT EXW-12) to the same short multi-path cell and FTS used in the CAVIAR measurements. One immediate advantage was that the spatial coherency of the SCLS led to an increased path-length through the cell (i.e. more reflections) from about 18 to 30 m.

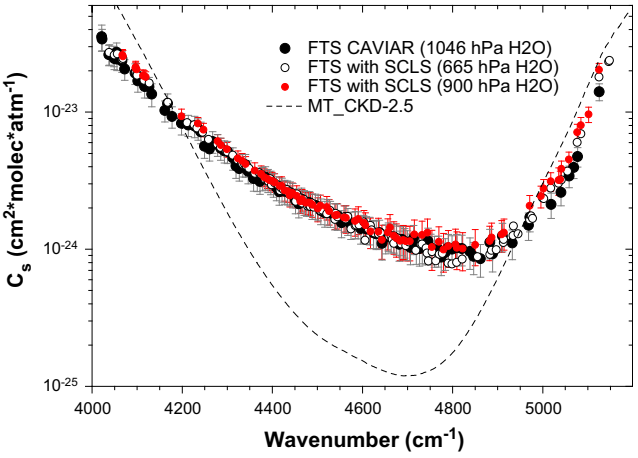

Fig. 9. Water vapour self-continuum cross-sections at about 400 K in the 4700 cm^{-1} window, retrieved from FTS measurements using a supercontinuum light source (SCLS), and compared with previous FTS CAVIAR measurements [23] with the same short-path absorption cell, but using a more conventional 50 W quartz tungsten halogen bulb result. The MT-CKD2.5 model continuum at 400 K is also shown.

Fig. 9 shows a comparison of the derived self-continuum (at 399 K, at 665 and 900 hPa vapour pressure) with the earlier CAVIAR (402 K, 1046 hPa) results in the 4700 cm^{-1} spectral region. The SCLS results are in excellent agreement with the earlier CAVIAR measurements; taken as a whole, the three measurements are consistent with the expected pressure-squared dependence of the self-continuum.

There are a number of challenges to a full efficient coupling of SCLS to an FTS. One of these is that SCLS are inherently noisy sources. It was not possible to derive the continuum in the 6300 cm^{-1} window in the pilot experiment, because of insufficient baseline stability. Indeed, while there was an order of magnitude improvement in source brightness, this improvement was not observed in the SNR due to greater excess noise compared to halogen lamps. To achieve a stable background signal, two options have been identified: to implement a feedback loop to stabilize the SCLS power output to better than 0.5%, and/or the development of a real-time baseline referencing through dual-channel detection. The latter solution would be highly efficient in removing instrumental drifts, though baseline drift due to multi-pass cell mechanical and thermal variation would still remain.

As an alternative to SCLS, superluminescent diodes (e.g. [81]) could be used as the FTS light source. These are readily available from >10,000 to ~6000 cm^{-1}. Typically they exhibit a broadband emission covering ~70 cm^{-1}, and a set of several sources could be multiplexed to investigate part of the 6300 cm^{-1} window.

4.2. Cavity-enhanced laser spectroscopy

An important advantage of FTS is its very wide spectral coverage. Laser methods now allow the coverage of wide spectral regions, in particular in the near-infrared, but at the expense of considerable effort. For instance, the Grenoble team has a collection of about 90 Distributed Feedback laser diodes (DFB) which allow a continuous coverage of the wide 5850–7920 cm^{-1} region (1.71–1.20 μm). DFB are also available at lower wavenumbers, but are less powerful, reducing to some extent the performance of the CRDS set-ups. Higher frequency regions are accessible with External Cavity Enhanced Laser diodes and continuum measurements by CRDS are planned in the 8000 cm^{-1} region. Because of the weak value of the continuum in this region, adsorbed water present on the mirror surface may play a role as evidenced in the 6100 cm^{-1} window [60]. To more precisely quantify the adsorbate contribution in order to more reliably derive the true self-continuum, Grenoble plan to develop a CRDS cavity with an adjustable length. This would allow the relative contribution of adsorbed water and water vapour to be varied while keeping the same set of super mirrors. In this context, additional CRDS (or OF-CEAS) measurements in other laboratories with set-ups using different cells and mirrors would be beneficial.

4.3. Other techniques

Other laser spectroscopy approaches would enable further independent measurement approaches. External cavity near-infrared laser sources are maturing and a few widely tuneable sources could cover the 6300 and the 4700 cm^{-1} windows with coarse tuning over a range of more than 400 cm^{-1}. Direct laser spectroscopy based on these sources, emitting a few mW of optical power, using high gain multi-pass cells, could provide a straightforward solution offering SNR improvement compared to FTS, without the stringent requirement on broadband high reflection coatings needed with cavity techniques.

In the medium term, spectroscopy approaches based on frequency combs may offer significant improvement. Spectrometers based on Fourier transform and direct absorption techniques have been proposed and demonstrated in the near-infrared [82,83].

Another potential technique for weak continuum measurement is high-sensitivity optoacoustic spectrometry (OAS) (e.g. [84–86]). The sensitivity of the OAS is proportional to the power of the laser used to generate the acoustic signal in the OA cell. Modern diode lasers with output power from 5 to 30 mW in combination with a two-channel OA cell [86] allow sensitivities at the 10^{-9} cm^{-1} level. Such sensitivity would be sufficient for detecting continuum absorption in the 4700 cm^{-1}, 6300 cm^{-1} and even the 8000 cm^{-1} windows if it is at the level of the room-temperature MT_CKD2.5 continuum. The OAS method has an even greater sensitivity for the foreign continuum when measurements are made at higher (around 1000 hPa) pressures. Nevertheless a drawback of OAS is that it requires calibration using a reference absorption signal.

4.4. Atmospheric measurements

The direct measurement of water vapour continuum absorption in the atmosphere is, ultimately, the most direct way of establishing its importance for the planetary radiation budget and remote sensing. There is a long history of such measurements, in the infrared and microwave where the continuum is stronger (e.g. [5,53,87–90]).

For the weaker near-infrared continuum, measurements are more difficult. Sierk et al. [91] report long-path DOAS retrievals of the continuum at wavenumber greater than 10,000 cm^{-1}. Pfeilsticker et al. [92], using a related approach, claimed the identification of a water dimer absorption feature around 13,400 cm^{-1}; subsequent laboratory [93,94] and theoretical [95] analyses raised serious doubts about this attribution.

There is potential for progress in the near-infrared bands using a variety of approaches. One is *via* sun-pointing high-resolution spectroscopy (e.g. Ref. [96]) in which continuum absorption can be retrieved directly, or *via* Langley analysis of the variation of surface irradiance with solar zenith angle (e.g. Ref. [97]). There are formidable problems in such analyses beyond those in properly characterising the instrument behaviour itself. These include the characterisation of the atmospheric state (vertical profiles of temperature, humidity, other gases, etc.); the greatest difficulty is aerosol scattering and absorption (and, potentially, the effect of thin undetected cloud), which is also of a continuum nature and which becomes more important at higher wavenumbers. A full characterisation of the aerosol impact is difficult using existing observations, and detailed sensitivity analyses are required. Direct use of solar irradiances is made more difficult because of a significant disagreement (of order 7%) on the incoming top-of-atmosphere near-infrared solar radiation from analyses of recent satellite measurements (e.g. Ref. [98]).

An alternative approach to using the sun as a source is using horizontal path measurements and laser sources. For example, Rieker et al. [99] demonstrate a frequency-comb spectroscopy technique over 2 km paths for the detection of CO_2 and CH_4 lines. Such approaches could be adapted for water vapour continuum measurements, but many of the difficulties in the sun-pointing approach would remain, and the shorter path lengths would make detection of continuum absorption more difficult.

4.5. Theoretical developments

Significant progress has been achieved in recent years both in water dimer theory and in developing links between theoretical predictions and new measurements, as discussed in Section 2.2. One key limitation of present analyses in the near-infrared is the

absence of calculations of the rotational structure of the dimer vibrational bands.

Section 2.2 also reported the first approaches to quantitative modelling of the contribution of bound and quasi-bound dimers to the self-continuum in near-infrared windows and it is important that these efforts are continued. Recent results appear to show that continuum absorption cannot be fully accounted for by the bound and quasi-bound components, and indicate the need for further theoretical developments. The analysis of experimental self-continuum spectra in the millimetre window [36] and the water vapour rotational band (see Tretyakov et al., http://symp.iao.ru/files/symp/hrms/18/presentation_7023.pdf) indicates that only about half of the self-continuum absorption could be attributed to bound and quasi-bound water dimers. This conclusion is reached using a total dimerization constant derived from the experimentally-derived second virial coefficient [100] or from *ab initio* calculations [101]. A similar result also follows from analysis of the self-continuum spectra in two strong near-IR absorption bands (Ptashnik and Klimeshina, http://symp.iao.ru/files/symp/hrms/18/presentation_7055.pdf). Because this unexplained absorption is present within bands and windows, it is unlikely that it can be attributed to the far wings of water monomer lines, although it may include a contribution from line absorption closer to the line centre.

Theoretical efforts aimed at understanding this unexplained absorption could include the development of the theory of spectral line "middle wings" and first-principle calculations accounting for absorption by quasi-bound dimers, for example, similar to the molecular dynamic approach reported by Ref. [102]. Theoretical partitioning of bound and quasi-bound H_2O–H_2O and H_2O–N_2 complexes based either on the molecular statistics approach developed in [30,42,103] (and using modern intermolecular potentials) or on direct trajectory calculations [104,105], could also be very helpful for clarifying the contribution of different components of bimolecular absorption to the water vapour continuum.

The variation of the temperature dependence of the continuum, both between windows, and as a function of temperature itself, has been highlighted in the measurements. The representation of the continuum in terms of a sum of contributions from bound and quasi-bound dimers [6,72] gives an insight into the possible physical origin of such complex temperature dependences. The simple exponential form $T^{2-n}\exp(D_0/kT)$ [45] should be reliable at low temperatures when absorption by bound dimers dominates. It may be not adequate at higher temperatures when quasi-bound dimers start to dominate the dimer population. The resulting T-dependence can then be a non-trivial combination of the bound- and quasi-bound dimer components (each having their own wavelength and T-dependence). Verification of this hypothesis requires more measurements over wider temperature regions and theoretical development on the expected spectral appearance of quasi-bound dimers in different spectral regions, as well as improved understanding of the unexplained absorption discussed above.

Finally, complexes beyond H_2O–H_2O and H_2O–N_2 (such as H_2O–O_2 and H_2O–Ar) have been proposed to contribute to the continuum (e.g. [31]) and would justify further examination both theoretically and in the laboratory.

Acknowledgments

The University of Reading and Rutherford-Appleton Laboratory acknowledge support from the UK Science and Technology Facilities Council (Grant ST/M000281/1) for a pilot project using a supercontinuum source. Gary Williams is thanked for his contribution to these measurements. The Grenoble group is supported by the LabexOSUG@2020 (ANR10 LABX56) and the LEFE-ChAt program from CNRS-INSU. IVP acknowledges support from the Russian Science Foundation (RSF project number 16-17-10096). Jon Elsey is thanked for his comments on the text. The critical comments of two reviewers were very valuable.

References

[1] N. Jacquinet-Husson, L. Crepeau, R. Armante, C. Boutammine, A. Chedin, N.A. Scott, C. Crevoisier, V. Capelle, C. Boone, N. Poulet-Crovisier, A. Barbe, A. Campargue, D.C. Benner, Y. Benilan, B. Bezard, V. Boudon, L.R. Brown, L.H. Coudert, A. Coustenis, V. Dana, V.M. Devi, S. Fally, A. Fayt, J.M. Flaud, A. Goldman, M. Herman, G.J. Harris, D. Jacquemart, A. Jolly, I. Kleiner, A. Kleinbohl, F. Kwabia-Tchana, N. Lavrentieva, N. Lacome, L.H. Xu, O.M. Lyulin, J. Y. Mandin, A. Maki, S. Mikhailenko, C.E. Miller, T. Mishina, N. Moazzen-Ahmadi, H.S.P. Muller, A. Nikitin, J. Orphal, V. Perevalov, A. Perrin, D.T. Petkie, A. Predoi-Cross, C.P. Rinsland, J.J. Remedios, M. Rotger, M.A.H. Smith, K. Sung, S. Tashkun, J. Tennyson, R.A. Toth, A.C. Vandaele, J. Vander Auwera, The edition of the GEISA spectroscopic database, J. Quant. Spectrosc. Radiat. Transfer 112 (2011) (2009) 2395–2445, http://dx.doi.org/10.1016/j.jqsrt.2011.06.004.

[2] L.S. Rothman, I.E. Gordon, Y. Babikov, A. Barbe, D.C. Benner, P.F. Bernath, M. Birk, L. Bizzocchi, V. Boudon, L.R. Brown, A. Campargue, K. Chance, E.A. Cohen, L.H. Coudert, V.M. Devi, B.J. Drouin, A. Fayt, J.M. Flaud, R.R. Gamache, J.J. Harrison, J.M. Hartmann, C. Hill, J.T. Hodges, D. Jacquemart, A. Jolly, J. Lamouroux, R.J. Le Roy, G. Li, D.A. Long, O.M. Lyulin, C.J. Mackie, S.T. Massie, S. Mikhailenko, H.S.P. Mueller, O.V. Naumenko, A.V. Nikitin, J. Orphal, V. Perevalov, A. Perrin, E.R. Polovtseva, C. Richard, M.A.H. Smith, E. Starikova, K. Sung, S. Tashkun, J. Tennyson, G.C. Toon, V.G. Tyuterev, G. Wagner, The HITRAN2012 molecular spectroscopic database, J. Quant. Spectrosc. Radiat. Transfer 130 (2013) 4–50, http://dx.doi.org/10.1016/j.jqsrt.2013.07.002.

[3] C. Richard, I.E. Gordon, L.S. Rothman, M. Abel, L. Frommhold, M. Gustafsson, J. M. Hartmann, C. Hermans, W.J. Lafferty, G.S. Orton, K.M. Smith, H. Tran, New section of the HITRAN database: collision-induced absorption (CIA), J. Quant. Spectrosc. Radiat. Transfer 113 (2012) 1276–1285, http://dx.doi.org/10.1016/j.jqsrt.2011.11.004.

[4] S.A. Clough, F.X. Kneizys, R.W. Davies, Line shape and the water vapor continuum, Atmos. Res. 23 (1989) 229–241, http://dx.doi.org/10.1016/0169-8095(89)90020-3.

[5] E.J. Mlawer, V.H. Payne, J.L. Moncet, J.S. Delamere, M.J. Alvarado, D.C. Tobin, Development and recent evaluation of the MT_CKD model of continuum absorption, Philos. Trans. Roy. Soc. A – Math. Phys. Eng. Sci. 370 (2012) 2520–2556, http://dx.doi.org/10.1098/rsta.2011.0295.

[6] I.V. Ptashnik, K.P. Shine, A.A. Vigasin, Water vapour self-continuum and water dimers: 1. Analysis of recent work, J. Quant. Spectrosc. Radiat. Transfer 112 (2011) 1286–1303, http://dx.doi.org/10.1016/j.jqsrt.2011.01.012.

[7] M.Y. Tretyakov, M.A. Koshelev, E.A. Serov, V.V. Parshin, T.A. Odintsova, G.M. Bubnov, Water dimer and the atmospheric continuum, Phys. Usp. 57 (2014) 1083–1098, http://dx.doi.org/10.3367/UFNr.0184.201411c.1199.

[8] A. Mukhopadhyay, W.T.S. Cole, R.J. Saykally, The water dimer I: experimental characterization, Chem. Phys. Lett. 633 (2015) 13–26, http://dx.doi.org/10.1016/j.cplett.2015.04.016.

[9] K.P. Shine, I.V. Ptashnik, G. Rädel, The water vapour continuum: brief history and recent developments, Surv. Geophys. 33 (2012) 535–555, http://dx.doi.org/10.1007/s10712-011-9170-y.

[10] S.A. Clough, M.J. Iacono, J.L. Moncet, Line-by-line calculations of atmospheric fluxes and cooling rates – application to water vapor, J. Geophys. Res. – Atmos. 97 (1992) 15761–15785.

[11] K.M. Firsov, T.Y. Chesnokova, Sensitivity of downward longwave radiative fluxes to water vapour continuum absorption, Atmos. Ocean. Opt. 23 (2010) 462–468, http://dx.doi.org/10.1134/S1024856010060059.

[12] S.M.S. Costa, K.P. Shine, Outgoing longwave radiation due to directly transmitted surface emission, J. Atmos. Sci. 69 (2012) 1865–1870, http://dx.doi.org/10.1175/jas-d-11-0248.1.

[13] K.J. Bignell, Water-vapour infra-red continuum, Quart. J. Roy. Meteorol. Soc. 96 (1970) 390, http://dx.doi.org/10.1002/qj.49709640904.

[14] D.E. Burch, R.L. Alt, Continuum Absorption by H_2O in the 700–1200 cm^{-1} and 2400–2800 cm^{-1} windows, Air Force Geophys. Lab, Hanscom AFB, Mass, 1984.

[15] W.R. Watkins, K.O. White, L.R. Bower, B.Z. Sojka, Pressure-dependence of the water-vapor continuum absorption in the 3.5–4.0 μm region, Appl. Opt. 18 (1979) 1149–1160, http://dx.doi.org/10.1364/ao.18.001149.

[16] Y.I. Baranov, W.J. Lafferty, The water-vapor continuum and selective absorption in the 3–5 μm spectral region at temperatures from 311 to 363 K, J. Quant. Spectrosc. Radiat. Transfer 112 (2011) 1304–1313, http://dx.doi.org/10.1016/j.jqsrt.2011.01.024.

[17] I.V. Ptashnik, R.A. McPheat, K.P. Shine, K.M. Smith, R.G. Williams, Water vapour foreign-continuum absorption in near-infrared windows from laboratory measurements, Philos. Trans. Roy. Soc. A – Math. Phys. Eng. Sci. 370 (2012) 2557–2577, http://dx.doi.org/10.1098/rsta.2011.0218.

[18] C. Frankenberg, R. Pollock, R.A.M. Lee, R. Rosenberg, J.F. Blavier, D. Crisp, C.W. O'Dell, G.B. Osterman, C. Roehl, P.O. Wennberg, D. Wunch, The Orbiting Carbon Observatory (OCO-2): spectrometer performance evaluation using

pre-launch direct sun measurements, Atmos. Meas. Tech. 8 (2015) 301–313, http://dx.doi.org/10.5194/amt-8-301-2015.
[19] H. Herbin, L.C. Labonnote, P. Dubuisson, Multispectral information from TANSO-FTS instrument – Part 1: application to greenhouse gases (CO_2 and CH_4) in clear sky conditions, Atmos. Meas. Tech. 6 (2013) 3301–3311, http://dx.doi.org/10.5194/amt-6-3301-2013.
[20] A. Galli, S. Guerlet, A. Butz, I. Aben, H. Suto, A. Kuze, N.M. Deutscher, J. Notholt, D. Wunch, P.O. Wennberg, D.W.T. Griffith, O. Hasekamp, J. Landgraf, The impact of spectral resolution on satellite retrieval accuracy of CO_2 and CH_4, Atmos. Meas. Tech. 7 (2014) 1105–1119, http://dx.doi.org/10.5194/amt-7-1105-2014.
[21] Z.B. Zhang, S. Platnick, An assessment of differences between cloud effective particle radius retrievals for marine water clouds from three MODIS spectral bands, J. Geophys. Res. – Atmos. 116 (2011) D20215, http://dx.doi.org/10.1029/2011jd016216.
[22] E.G. Moody, M.D. King, C.B. Schaaf, S. Platnick, MODIS-derived spatially complete surface albedo products: spatial and temporal pixel distribution and zonal averages, J. Appl. Meteorol. Climatol. 47 (2008) 2879–2894, http://dx.doi.org/10.1175/2008jamc1795.1.
[23] I.V. Ptashnik, R.A. McPheat, K.P. Shine, K.M. Smith, R.G. Williams, Water vapor self-continuum absorption in near-infrared windows derived from laboratory measurements, J. Geophys. Res. – Atmos. 116 (2011) D16305, http://dx.doi.org/10.1029/2011JD015603.
[24] D.J. Paynter, I.V. Ptashnik, K.P. Shine, K.M. Smith, R. McPheat, R.G. Williams, Laboratory measurements of the water vapor continuum in the 1200–8000 cm^{-1} region between 293 K and 351 K, J. Geophys. Res. – Atmos. 114 (2009) D21301, http://dx.doi.org/10.1029/2008JD011355.
[25] Q. Ma, R.H. Tipping, A far-wing line-shape theory and its application to the water continuum absorption in the infrared region 1, J. Chem. Phys. 95 (1991) 6290–6301, http://dx.doi.org/10.1063/1.461549.
[26] Q. Ma, R.H. Tipping, C. Leforestier, Temperature dependences of mechanisms responsible for the water-vapor continuum absorption. I. Far wings of allowed lines, J. Chem. Phys. 128 (2008) 124313, http://dx.doi.org/10.1063/1.2839604.
[27] S.D. Tvorogov, O.B. Rodimova, Spectral line shape 1. Kinetic equation for arbitrary frequency detunings, J. Chem. Phys. 102 (1995) 8736–8745, http://dx.doi.org/10.1063/1.468977.
[28] J.V. Bogdanova, O.B. Rodimova, Line shape in far wings and water vapor absorption in a broad temperature interval, J. Quant. Spectrosc. Radiat. Transfer 111 (2010) 2298–2307, http://dx.doi.org/10.1016/j.jqsrt.2010.05.005.
[29] O.B. Rodimova, Spectral line shape and absorption in atmospheric windows, Atmos. Ocean. Opt. 28 (2015) 460–473 (in Russian).
[30] A.A. Vigasin, Bound, metastable and free states of bimolecular complexes, Infrared Phys. 32 (1991) 461–470, http://dx.doi.org/10.1016/0020-0891(91)90135-3.
[31] H.G. Kjaergaard, T.W. Robinson, D.L. Howard, J.S. Daniel, J.E. Headrick, V. Vaida, Complexes of importance to the absorption of solar radiation, J. Phys. Chem. A 107 (2003) 10680–10686, http://dx.doi.org/10.1021/jp035098t.
[32] K.H. Lemke, T.M. Seward, Ab initio investigation of the structure, stability, and atmospheric distribution of molecular clusters containing H_2O, CO_2, and N_2O, J. Geophys. Res. – Atmos. 113 (2008) D19304, http://dx.doi.org/10.1029/2007jd009148.
[33] Y. Scribano, C. Leforestier, Contribution of water dimer absorption to the millimeter and far infrared atmospheric water continuum, J. Chem. Phys. 126 (2007) 234301, http://dx.doi.org/10.1063/1.2746038.
[34] H.G. Kjaergaard, A.L. Garden, G.M. Chaban, R.B. Gerber, D.A. Matthews, J.F. Stanton, Calculation of vibrational transition frequencies and intensities in water dimer: comparison of different vibrational approaches, J. Phys. Chem. A 112 (2008) 4324–4335, http://dx.doi.org/10.1021/jp710066f.
[35] T. Salmi, V. Haenninen, A.L. Garden, H.G. Kjaergaard, J. Tennyson, L. Halonen, Calculation of the O-H stretching vibrational overtone spectrum of the water dimer, J. Phys. Chem. A 112 (2008) 6305–6312, http://dx.doi.org/10.1021/jp800754y.
[36] E.A. Serov, M.A. Koshelev, T.A. Odintsova, V.V. Parshin, M.Y. Tretyakov, Rotationally resolved water dimer spectra in atmospheric air and pure water vapour in the 188–258 GHz range, Phys. Chem. Chem. Phys. 16 (2014) 26221–26233, http://dx.doi.org/10.1039/c4cp03252g.
[37] M.Y. Tretyakov, E.A. Serov, M.A. Koshelev, V.V. Parshin, A.F. Krupnov, Water dimer rotationally resolved millimeter-wave spectrum: observation at room temperature, Phys. Rev. Lett. 110 (2013) 093001, http://dx.doi.org/10.1103/PhysRevLett. 110.093001.
[38] I.V. Ptashnik, K.M. Smith, K.P. Shine, D.A. Newnham, Laboratory measurements of water vapour continuum absorption in spectral region 5000–5600 cm^{-1}: evidence for water dimers, Quart. J. Roy. Meteorol. Soc. 130 (2004) 2391–2408, http://dx.doi.org/10.1256/qj.03.178.
[39] I.V. Ptashnik, Evidence for the contribution of water dimers to the near-IR water vapour self-continuum, J. Quant. Spectrosc. Radiat. Transfer 109 (2008) 831–852, http://dx.doi.org/10.1016/j.jqsrt.2007.09.004.
[40] D.J. Paynter, I.V. Ptashnik, K.P. Shine, K.M. Smith, Pure water vapor continuum measurements between 3100 and 4400 cm^{-1}: evidence for water dimer absorption in near atmospheric conditions, Geophys. Res. Lett. 34 (2007) L12808, http://dx.doi.org/10.1029/2007GL029259.
[41] A.A. Vigasin, Bimolecular absorption in atmospheric gases, Weakly Interacting Molecular Pairs: Unconventional Absorbers of Radiation in the Atmosphere, Kluwer Academic Publishers, 2003, pp. 23–47.
[42] S.Y. Epifanov, A.A. Vigasin, Subdivision of phase space for anisotropically interacting water molecules, Mol. Phys. 90 (1997) 101–106, http://dx.doi.org/10.1080/002689797172912.
[43] G.K. Schenter, S.M. Kathmann, B.C. Garrett, Equilibrium constant for water dimerization: analysis of the partition function for a weakly bound system, J. Phys. Chem. A 106 (2002) 1557–1566, http://dx.doi.org/10.1021/jp0129131.
[44] J.S. Daniel, S. Solomon, H.G. Kjaergaard, D.P. Schofield, Atmospheric water vapor complexes and the continuum, Geophys. Res. Lett. 31 (2004) L06118, http://dx.doi.org/10.1029/2003gl018914.
[45] A.A. Vigasin, Water vapor continuous absorption in various mixtures: possible role of weakly bound complexes, J. Quant. Spectrosc. Radiat. Transfer 64 (2000) 25–40, http://dx.doi.org/10.1016/s0022-4073(98)00142-3.
[46] J.G. Cormier, J.T. Hodges, J.R. Drummond, Infrared water vapor continuum absorption at atmospheric temperatures, J. Chem. Phys. 122 (2005) 114309, http://dx.doi.org/10.1063/1.1862623.
[47] A. Bauer, M. Godon, Continuum for H_2O-X mixtures in the H_2O spectral window at 239 GHz; X = C_2H_4, C_2H_6 – are collision-induced absorption processes involved?, J Quant. Spectrosc. Radiat. Transfer 69 (2001) 277–290, http://dx.doi.org/10.1016/s0022-4073(00)00080-7.
[48] Y.I. Baranov, W.J. Lafferty, The water vapour self- and water-nitrogen continuum absorption in the 1000 and 2500 cm^{-1} atmospheric windows, Philos. Trans. Roy. Soc. A – Math. Phys. Eng. Sci. 370 (2012) 2578–2589, http://dx.doi.org/10.1098/rsta.2011.0234.
[49] A.A. Vigasin, Water vapor continuum: whether collision-induced absorption is involved?, J Quant. Spectrosc. Radiat. Transfer 148 (2014) 58–64, http://dx.doi.org/10.1016/j.jqsrt.2014.06.019.
[50] A.A. Vigasin, Collision-induced absorption in the region of the O_2 fundamental: bandshapes and dimeric features, J. Mol. Spectrosc. 202 (2000) 59–66, http://dx.doi.org/10.1006/jmsp.2000.8094.
[51] A.A. Vigasin, Y.I. Baranov, G.V. Chlenova, Temperature variations of the interaction induced absorption of CO_2 in the ν_1, $2\nu_2$ region: FTIR measurements and dimer contribution, J. Mol. Spectrosc. 213 (2002) 51–56, http://dx.doi.org/10.1006/jmsp.2002.8529.
[52] J. Hinderling, M.W. Sigrist, F.K. Kneubuhl, Laser photoacoustic spectroscopy of water-vapor continuum and line absorption in the 8 μm and 14 μm atmospheric window, Infrared Phys. 27 (1987) 63–120, http://dx.doi.org/10.1016/0020-0891(87)90013-3.
[53] J.P. Taylor, S.M. Newman, T.J. Hewison, A. McGrath, Water vapour line and continuum absorption in the thermal infrared – reconciling models and observations, Quart. J. Roy. Meteorol. Soc. 129 (2003) 2949–2969, http://dx.doi.org/10.1256/qj.03.08.
[54] Y.I. Baranov, W.J. Lafferty, Q. Ma, R.H. Tipping, Water-vapor continuum absorption in the 800–1250 cm^{-1} spectral region at temperatures from 311 to 363 K, J. Quant. Spectrosc. Radiat. Transfer 109 (2008) 2291–2302, http://dx.doi.org/10.1016/j.jqsrt.2008.03.004.
[55] I.V. Ptashnik, T.M. Petrova, Y.N. Ponomarev, K.P. Shine, A.A. Solodov, A.M. Solodov, Near-infrared water vapour self-continuum at close to room temperature, J. Quant. Spectrosc. Radiat. Transfer 120 (2013) 23–35, http://dx.doi.org/10.1016/j.jqsrt.2013.02.016.
[56] S.F. Fulghum, M.M. Tilleman, Interferometric calorimeter for the measurement of water-vapor absorption, J. Opt. Soc. Am. B – Opt. Phys. 8 (1991) 2401–2413, http://dx.doi.org/10.1364/josab.8.002401.
[57] I.V. Ptashnik, T.M. Petrova, Y.N. Ponomarev, A.A. Solodov, A.M. Solodov, Water vapor continuum absorption in near-IR atmospheric windows, Atmos. Ocean. Opt. 28 (2015) 115–120, http://dx.doi.org/10.1134/S102485601502009.
[58] I. Ventrillard, D. Romanini, D. Mondelain, A. Campargue, Accurate measurements and temperature dependence of the water vapor self-continuum absorption in the 2.1 μm atmospheric window, J. Chem. Phys. 143 (2015) 134304, http://dx.doi.org/10.1063/1.4931811.
[59] D. Mondelain, S. Vasilchenko, P. Cermak, S. Kassi, A. Campargue, The self- and foreign-absorption continua of water vapor by cavity ring-down spectroscopy near 2.35 μm, Phys. Chem. Chem. Phys. 17 (2015) 17762–17770, http://dx.doi.org/10.1039/c5cp01238d.
[60] D. Mondelain, S. Manigand, S. Kassi, A. Campargue, Temperature dependence of the water vapor self-continuum by cavity ring-down spectroscopy in the 1.6 μm transparency window, J. Geophys. Res. – Atmos. 119 (2014) 5625–5639, http://dx.doi.org/10.1002/2013jd021319.
[61] D. Mondelain, A. Aradj, S. Kassi, A. Campargue, The water vapour self-continuum by CRDS at room temperature in the 1.6 μm transparency window, J. Quant. Spectrosc. Radiat. Transfer 130 (2013) 381–391, http://dx.doi.org/10.1016/j.jqsrt.2013.07.006.
[62] W.E. Bicknell, S.D. Cecca, M.K. Griffin, Search for low-absorption regimes in the 1.6 and 2.1 μm atmospheric windows, J. Direct. Energy 2 (2006) 151–161.
[63] D. Romanini, A.A. Kachanov, N. Sadeghi, F. Stoeckel, CW cavity ring down spectroscopy, Chem. Phys. Lett. 264 (1997) 316–322, http://dx.doi.org/10.1016/s0009-2614(96)01351-6.
[64] G. Berden, R. Peeters, G. Meijer, Cavity ring-down spectroscopy: experimental schemes and applications, Int. Rev. Phys. Chem. 19 (2000) 565–607, http://dx.doi.org/10.1080/014423500750040627.
[65] S. Kassi, A. Campargue, Cavity ring down spectroscopy with 5×10^{-13} cm^{-1} sensitivity, J. Chem. Phys. 137 (2012) 234201, http://dx.doi.org/10.1063/1.4769974.
[66] D. Romanini, M. Chenevier, S. Kassi, M. Schmidt, C. Valant, M. Ramonet, J. Lopez, H.J. Jost, Optical-feedback cavity-enhanced absorption: a compact spectrometer for real-time measurement of atmospheric methane, Appl.

Phys. B – Lasers Opt. 83 (2006) 659–667, http://dx.doi.org/10.1007/s00340-006-2177-2.
[67] J. Morville, S. Kassi, M. Chenevier, D. Romanini, Fast, low-noise, mode-by-mode, cavity-enhanced absorption spectroscopy by diode-laser self-locking, Appl. Phys. B – Lasers Opt. 80 (2005) 1027–1038, http://dx.doi.org/10.1007/s00340-005-1828-z.
[68] E.R.T. Kerstel, R.Q. Iannone, M. Chenevier, S. Kassi, H.J. Jost, D. Romanini, A water isotope (^{2}H, ^{17}O, and ^{18}O) spectrometer based on optical feedback cavity-enhanced absorption for in situ airborne applications, Appl. Phys. B – Lasers Opt. 85 (2006) 397–406, http://dx.doi.org/10.1007/s00340-006-2356-1.
[69] R.H. Tipping, Q. Ma, Theory of water-vapor continuum and validations, Atmos. Res. 36 (1995) 69–94, http://dx.doi.org/10.1016/0169-8095(94)00028-c.
[70] D. Paynter, V. Ramaswamy, Variations in water vapor continuum radiative transfer with atmospheric conditions, J. Geophys. Res. – Atmos. 117 (2012) D16310, http://dx.doi.org/10.1029/2012jd017504.
[71] D. Paynter, V. Ramaswamy, Investigating the impact of the shortwave water vapor continuum upon climate simulations using GFDL global models, J. Geophys. Res. – Atmos. 119 (2014) 10720–10737, http://dx.doi.org/10.1002/2014jd021881.
[72] A. Pavlyuchko, A. Vigasin, The water dimer anharmonicity and the water-vapor continuum absorption, in: The 20th International Conference on High Resolution Molecular Spectroscopy, Prague, Czech Republic, 2008, p. 147.
[73] J.M. Hartmann, M.Y. Perrin, Q. Ma, R.H. Tipping, The infrared continuum of pure water vapor – calculations and high-temperature measurements, J. Quant. Spectrosc. Radiat. Transfer 49 (1993) 675–691, http://dx.doi.org/10.1016/0022-4073(93)90010-f.
[74] D.E. Burch, Continuum Absorption by H_2O, Air Force Geophysics Laboratory Report, Hanscom AFB, MA, 1981.
[75] Y.I. Baranov, The continuum absorption in $H_2O + N_2$ mixtures in the 2000–3250 cm^{-1} spectral region at temperatures from 326 to 363 K, J. Quant. Spectrosc. Radiat. Transfer 112 (2011) 2281–2286, http://dx.doi.org/10.1016/j.jqsrt.2011.06.005.
[76] G. Rädel, K.P. Shine, I.V. Ptashnik, Global radiative and climate effect of the water vapour continuum at visible and near-infrared wavelengths, Quart. J. Roy. Meteorol. Soc. 141 (2015) 727–738, http://dx.doi.org/10.1002/qj.2385.
[77] R. Thapa, D. Rhonehouse, D. Nguyen, K. Wiersma, C. Smith, J. Zong, A. Chavez-Pirson, Mid-IR supercontinuum generation in ultra-low loss, dispersion-zero shifted tellurite glass fiber with extended coverage beyond 4.5 μm, in: D.H. Titterton, M.A. Richardson, R.J. Grasso, H. Ackermann, W.L. Bohn (Eds.), Technologies for Optical Countermeasures X; and High-Power Lasers 2013: Technology and Systems, 2013.
[78] D.R. Herriot, H.J. Schulte, Folded optical delay lines, Appl. Opt. 4 (1965) 883–889, http://dx.doi.org/10.1364/AO.4.000883.
[79] J.B. McManus, P.L. Kebabian, W.S. Zahniser, Astigmatic mirror multipass absorption cells for long-path-length spectroscopy, Appl. Opt. 34 (1995) 3336–3348, http://dx.doi.org/10.1364/AO.34.003336.
[80] J. Orphal, A.A. Ruth, High-resolution Fourier-transform cavity-enhanced absorption spectroscopy in the near-infrared using an incoherent broadband light source, Opt. Express 16 (2008) 19232–19243, http://dx.doi.org/10.1364/oe.16.019232.
[81] A. Aalto, G. Genty, T. Laurila, J. Toivonen, Incoherent broadband cavity enhanced absorption spectroscopy using supercontinuum and superluminescent diode sources, Opt. Express 23 (2015) 25225–25234, http://dx.doi.org/10.1364/oe.23.025225.
[82] J. Mandon, G. Guelachvili, N. Picque, Fourier transform spectroscopy with a laser frequency comb, Nat. Photonics 3 (2009) 99–102, http://dx.doi.org/10.1038/nphoton.2008.293.
[83] N.R. Newbury, I. Coddington, W. Swann, Sensitivity of coherent dual-comb spectroscopy, Opt. Express 18 (2010) 7929–7945, http://dx.doi.org/10.1364/oe.18.007929.
[84] A.B. Tikhomirov, I.V. Ptashnik, B.A. Tikhomirov, Measurement of the continuum absorption coefficient of water vapor near 14400 cm^{-1} (0.694 μm), Opt. Spectrosc. 101 (2006) 80–89, http://dx.doi.org/10.1134/s0030400x06070150.
[85] I.V. Ptashnik, V.A. Kapitanov, Y.N. Ponomarev, N.P. Krivolutski, S.M. Kobtsev, S.I. Kablukov, Determination of water vapor continuum absorption coefficient in 0.900 μm spectral range, Atmos. Ocean. Opt. 19 (2006) 614–616.
[86] V.A. Kapitanov, K.Y. Osipov, A.E. Protasevich, Y.N. Ponomarev, Collisional parameters of N_2 broadened methane lines in the R9 multiplet of the $2\nu_3$ band. Multispectrum fittings of the overlapping spectral lines, J. Quant. Spectrosc. Radiat. Transfer 113 (2012) 1985–1992, http://dx.doi.org/10.1016/j.jqsrt.2012.07.011.
[87] C. Serio, G. Masiello, F. Esposito, P. Di Girolamo, T. Di Iorio, L. Palchetti, G. Bianchini, G. Muscari, G. Pavese, R. Rizzi, B. Carli, V. Cuomo, Retrieval of foreign-broadened water vapor continuum coefficients from emitted spectral radiance in the H_2O rotational band from 240 to 590 cm^{-1}, Opt. Express 16 (2008) 15816–15833, http://dx.doi.org/10.1364/oe.16.015816.
[88] G. Liuzzi, G. Masiello, C. Serio, L. Palchetti, G. Bianchini, Validation of H_2O continuum absorption models in the wave number range 180–600 cm^{-1} with atmospheric emitted spectral radiance measured at the Antarctica Dome-C site, Opt. Express 22 (2014) 16784–16801, http://dx.doi.org/10.1364/oe.22.016784.
[89] S.M. Newman, P.D. Green, I.V. Ptashnik, T.D. Gardiner, M.D. Coleman, R.A. McPheat, K.M. Smith, Airborne and satellite remote sensing of the mid-infrared water vapour continuum, Philos. Trans. Roy. Soc. A – Math. Phys. Eng. Sci. 370 (2012) 2611–2636, http://dx.doi.org/10.1098/rsta.2011.0223.
[90] P.D. Green, S.M. Newman, R.J. Beeby, J.E. Murray, J.C. Pickering, J.E. Harries, Recent advances in measurement of the water vapour continuum in the far-infrared spectral region, Philos. Trans. Roy. Soc. A – Math. Phys. Eng. Sci. 370 (2012) 2637–2655, http://dx.doi.org/10.1098/rsta.2011.0263.
[91] B. Sierk, S. Solomon, J.S. Daniel, R.W. Portmann, S.I. Gutman, A.O. Langford, C. S. Eubank, E.G. Dutton, K.H. Holub, Field measurements of water vapor continuum absorption in the visible and near-infrared, J. Geophys. Res. – Atmos. 109 (2004) D08307, http://dx.doi.org/10.1029/2003jd003586.
[92] K. Pfeilsticker, A. Lotter, C. Peters, H. Bosch, Atmospheric detection of water dimers via near-infrared absorption, Science 300 (2003) 2078–2080, http://dx.doi.org/10.1126/science.1082282.
[93] S. Kassi, P. Macko, O. Naumenko, A. Campargue, The absorption spectrum of water near 750 nm by CW-CRDS: contribution to the search of water dimer absorption, Phys. Chem. Chem. Phys. 7 (2005) 2460–2467, http://dx.doi.org/10.1039/b502172c.
[94] A.J.L. Shillings, S.M. Ball, M.J. Barber, J. Tennyson, R.L. Jones, An upper limit for water dimer absorption in the 750 nm spectral region and a revised water line list, Atmos. Chem. Phys. 11 (2011) 4273–4287, http://dx.doi.org/10.5194/acp-11-4273-2011.
[95] A.L. Garden, L. Halonen, H.G. Kjaergaard, Calculated band profiles of the OH-stretching transitions in water dimer, J. Phys. Chem. A 112 (2008) 7439–7447, http://dx.doi.org/10.1021/jp802001g.
[96] T.D. Gardiner, M. Coleman, H. Browning, L. Tallis, I.V. Ptashnik, K.P. Shine, Absolute high spectral resolution measurements of surface solar radiation for detection of water vapour continuum absorption, Philos. Trans. Roy. Soc. A – Math. Phys. Eng. Sci. 370 (2012) 2590–2610, http://dx.doi.org/10.1098/rsta.2011.0221.
[97] L. Harrison, P. Kiedron, J. Berndt, J. Schlemmer, Extraterrestrial solar spectrum 360–1050 nm from Rotating Shadowband Spectroradiometer measurements at the Southern Great Plains (ARM) site, J. Geophys. Res. – Atmos. 108 (2003) 4424, http://dx.doi.org/10.1029/2001jd001311.
[98] M. Weber, Comment on the Article by Thuillier et al. "The Infrared Solar Spectrum Measured by the SOLSPEC Spectrometer onboard the International Space Station", Sol. Phys. 290 (2015) 1601–1605, http://dx.doi.org/10.1007/s11207-015-0707-y.
[99] G.B. Rieker, F.R. Giorgetta, W.C. Swann, J. Kofler, A.M. Zolot, L.C. Sinclair, E. Baumann, C. Cromer, G. Petron, C. Sweeney, P.P. Tans, I. Coddington, N.R. Newbury, Frequency-comb-based remote sensing of greenhouse gases over kilometer air paths, Optica 1 (2014) 290–298, http://dx.doi.org/10.1364/optica.1.000290.
[100] M.Y. Tretyakov, E.A. Serov, T.A. Odintsova, Equilibrium thermodynamic state of water vapor and the collisional interactions of molecules, Radiophys. Quantum Electron. 54 (2012) 700–716.
[101] C. Leforestier, Water dimer equilibrium constant calculation: a quantum formulation including metastable states, J. Chem. Phys. 140 (2014) 074106, http://dx.doi.org/10.1063/1.4865339.
[102] M.-S. Lee, F. Baletto, D.G. Kanhere, S. Scandolo, Far-infrared absorption of water clusters by first-principles molecular dynamics, J. Chem. Phys. 128 (2008) 214506, http://dx.doi.org/10.1063/1.2933248.
[103] A.A. Vigasin, On the nature of collision-induced absorption in gaseous homonuclear diatomics, J. Quant. Spectrosc. Radiat. Transfer 56 (1996) 409–422, http://dx.doi.org/10.1016/0022-4073(96)84530-4.
[104] S.E. Lokshtanov, S.V. Ivanov, A.A. Vigasin, Statistical physics partitioning and classical trajectory analysis of the phase space in CO_2-Ar weakly interacting pairs, J. Mol. Struct. 742 (2005) 31–36, http://dx.doi.org/10.1016/j.molstruc.2004.12.055.
[105] S.V. Ivanov, Trajectory study of CO_2-Ar and CO_2-He collision complexes, in: C. CamyPeyret, A.A. Vigasin (Eds.), Weakly Interacting Molecular Pairs: Unconventional Absorbers of Radiation in the Atmosphere, Kluwer Academic Publishers, 2003, pp. 49–63.